

SOUTHWEST RESEARCH INSTITUTE®

6220 CULEBRA ROAD • POST OFFICE DRAWER 28510 • SAN ANTONIO, TEXAS, USA 78228-0510 • (210) 684-5111 • TELEX 244846

ENGINE, EMISSIONS, AND VEHICLE RESEARCH DIVISION

ISO 9001 Certified

FAX: (210) 522-2019

ISO 14001 Certified

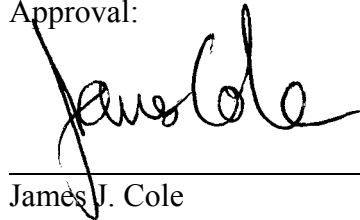
April 19, 2004

Mr. Richard Baker
U.S. Department of Energy
National Energy Technology Laboratory
3610 Collins Ferry Road, P.O. Box 880
Morgantown, WV 26507-0880
richard.baker@netl.doe.gov

Dear Mr. Baker:

Attached is the mid-term Technical Progress Report (revised) for DOE Contract No. DE-FC26-03NT41859; SwRI Project No. 03.10198 entitled "*Advanced Compressor Engine Controls to Enhance Operation, Reliability and Integrity.*" If you have any questions or comments, please feel free to contact me by telephone at 210-522-3131, by email at gbourn@swri.org, or by facsimile at 210-522-2019.

Approval:



James J. Cole
Assistant Director
Dept. of Engine & Emissions Research
Engine, Emission & Vehicle Research Div.

Respectfully submitted by:



Gary D. Bourn
Sr. Research Engineer
Dept. of Engine & Emissions Research
Engine, Emission & Vehicle Research Div.

/mr

Enclosure



SAN ANTONIO, TEXAS
HOUSTON, TEXAS ! WASHINGTON, DC

Advanced Compressor Engine Controls to Enhance Operation, Reliability and Integrity

Semi-Annual Technical Progress Report

Reporting Period Start Date: 09/22/03

Reporting Period End Date: 03/21/04

Principal Author:

Gary D. Bourn

April 2004

DOE Award No. DE-FC26-03NT41859

SwRI Project No. 03.10198

Submitting Organization:

Southwest Research Institute®

6220 Culebra Road

San Antonio, TX 78238-5166

DISCLAIMER

“This report was prepared as an account of work sponsored by an agency of the United States Government. Neither the United States Government nor any agency thereof, nor any of their employees, makes an warranty, express or implied, or assumes any legal liability or responsibility for the accuracy, completeness, or usefulness of any information, apparatus, product, or process disclosed, or represents that its use would not infringe privately owned rights. Reference herein to any specific commercial product, process, or service by trade name, trademark, manufacturer, or otherwise does not necessarily constitute or imply its endorsement, recommendation, or favoring by the United States Government or any agency thereof. The views and opinions of authors expressed herein do not necessarily state or reflect those of the United States Government or any agency thereof.”

ABSTRACT

This document provides a mid-term update for the “Advanced Compressor Engine Controls to Enhance Operation, Reliability, and Integrity” project. SwRI is conducting this project for DOE in conjunction with Cooper Energy Services, under DOE contract number DE-FC26-03NT41859. This report addresses the current status of engine controls for integral compressor engines and how they compare among each other.

EXECUTIVE SUMMARY

This document provides a mid-term update for the “Advanced Compressor Engine Controls to Enhance Operation, Reliability, and Integrity” project. SwRI is conducting this project for DOE in conjunction with Cooper Energy Services, under DOE contract number DE-FC26-03NT41859. The objective of this one-year project is to develop, evaluate, and demonstrate advanced engine control technologies and hardware, specifically, closed-loop NO_x emissions control on a two-stroke integral reciprocating engine/compressor used for pipeline gas transmission service. This work uses a Cooper-Bessemer GMVH-6 laboratory engine owned by Cooper Energy Services (CES) and installed in a test facility at Southwest Research Institute (SwRI).

The gas transmission industry operates over 4,000 integral engine compressors, the majority being two-stroke, with a median age of 45 years and a median size of 2000 horsepower. These engines have historically exhibited poor performance and high emissions, due in part to poor engine control. The end results are misfires and partial burns that lead to increased fuel usage and exhaust emissions. Many of the slow-speed integral engines in the gas compression industry utilize control systems that are outdated, slow, and suffer from poor resolution.

Research into more advanced control systems for integral compressor engines has increased tremendously in recent years. The recent advancements in control logic are being reviewed and analyzed in this program to understand the effectiveness of each. In addition, the application of a real-time NO_x sensor feedback for closed-loop control is being investigated. To date, the strategies involving fuel/air equivalence ratio for a NO_x prediction algorithm have been reviewed and analyzed.

A hierarchy of control strategies will be outlined at the conclusion of this program. This hierarchy will range from the simplest and least expensive closed-loop control to an advanced system utilizing individual cylinder control. The ultimate control strategy is thought to be one that integrates both compressor and engine control, with the engine control based on individual power cylinders. The hierarchy of engine control may be desirable for the variety of engines in various locations that are subject to varying regulated levels of NO_x emissions. The engines in non-attainment areas will require the maximum level of complexity in engine controls.

TABLE OF CONTENTS

		<u>Page</u>
1.	INTRODUCTION	1
2.	OBJECTIVE	1
3.	BACKGROUND	1
4.	TWO-STROKE INTEGRAL COMPRESSOR ENGINES	2
5.	ENGINE CONTROL FUNDAMENTALS	4
5.1	CONTROL CATEGORIES	4
5.2	FUEL/AIR EQUIVALENCE RATIO	6
5.2.1	<i>Equivalence Ratio from Emissions</i>	9
5.3	TWO-STROKE ENGINE EQUIVALENCE RATIO	10
5.3.1	<i>Trapping Efficiency Technique</i>	10
5.3.2	<i>Ideal Gas Law Technique</i>	13
5.4	NO _x EMISSIONS.....	14
5.5	NGK-LOCKE COMBINED NO _x /O ₂ SENSOR	18
6.	COMPRESSOR ENGINE CONTROLS	20
6.1	FUEL-AIR CURVE.....	20
6.2	CORRECTED AMP SETPOINT	21
6.3	TRAPPED EQUIVALENCE RATIO	21
6.4	CYLINDER PRESSURE BASED PEMS	22
6.5	INTEGRATED ENGINE-COMPRESSOR CONTROLS	22
6.6	ENABLING TECHNOLOGY	23
7.	RESULTS AND DISCUSSIONS	24
7.1	MASS AIRFLOW AND TRAPPED AIR MASS	24
7.2	TRAPPED EQUIVALENCE RATIO	28
7.3	NO _x PREDICTION FROM TRAPPED EQUIVALENCE RATIO	30
7.4	MODIFIED FUEL-AIR CURVE.....	33
7.5	CYLINDER PRESSURE BASED NO _x PREDICTION.....	33
7.6	INDIVIDUAL CYLINDER BASED STRATEGIES	34
8.	CONCLUSIONS	34

LIST OF TABLES

	<u>Page</u>
TABLE 5.1. EXAMPLE NATURAL GAS COMPOSITION AND STOICHIOMETRIC A/F RATIO	7
TABLE 5.2. RATE COEFFICIENTS FOR THE THERMAL NO MECHANISM.....	16
TABLE 7.1. REGRESSION STATISTICS FOR EQUIVALENCE RATIO BASED NO _x PREDICTION	33

LIST OF FIGURES

	<u>Page</u>
FIGURE 4.1. CROSS SECTION OF A COOPER-BESSEMER GMVH INTEGRAL COMPRESSOR ENGINE ..3	
FIGURE 4.2. TYPICAL INTEGRAL COMPRESSOR ENGINE CONTROL SYSTEM LAYOUT	4
FIGURE 5.1. TERMINOLOGY AND BASIC STRUCTURE OF A FEEDBACK CONTROL SYSTEM [1].....	5
FIGURE 5.2. TYPICAL SPARK-IGNITED LEAN-BURN OPERATING LIMIT FOR STEADY SPEED & LOAD8	
FIGURE 5.3. EXHAUST EMISSIONS VERSUS EQUIVALENCE RATIO [2].....	15
FIGURE 5.4. PHOTOGRAPH OF NGK-LOCKE COMBINED NO _x /O ₂ SENSOR.....	19
FIGURE 5.5. CALIBRATION OF NGK-LOCKE NO _x SIGNAL ON GMVH-6 ENGINE.....	19
FIGURE 5.6. CALIBRATION OF NGK-LOCKE UEGO SIGNAL ON GMVH-6 ENGINE	20
FIGURE 6.1. EXAMPLE FUEL-AIR CURVE	21
FIGURE 7.1. COMPARISON OF DRY TOTAL MASS AIRFLOWS FROM EMISSIONS AND ASME NOZZLE MEASUREMENTS.....	25
FIGURE 7.2. COMPARISON OF DRY TOTAL MASS AIRFLOW FROM EMISSIONS AND MODELED TOTAL MASS AIRFLOW.....	26
FIGURE 7.3. COMPARISON OF FLOW COEFFICIENT DERIVED FROM MEASURED AIRFLOW AND PREDICTED FROM REGRESSION MODEL	27
FIGURE 7.4. COMPARISON OF DRY TRAPPED MASS AIRFLOWS FROM TRAPPING EFFICIENCY AND IDEAL GAS BASED CALCULATIONS.....	28
FIGURE 7.5. COMPARISON OF ESTIMATED TRAPPING EFFICIENCIES.....	29
FIGURE 7.6. ESTIMATED TRAPPED EQUIVALENCE RATIOS USING THE TRAPPING EFFICIENCY BASED METHOD.....	29
FIGURE 7.7. ESTIMATED TRAPPED EQUIVALENCE RATIOS USING THE IDEAL GAS BASED METHOD30	
FIGURE 7.8. COMPARISON OF PREDICTED VERSUS MEASURED NO _x WITH GLOBAL EQUIVALENCE RATIO REGRESSION	31
FIGURE 7.9. COMPARISON OF PREDICTED VERSUS MEASURED NO _x WITH TRAPPED EQUIVALENCE RATIO (TRAPPING EFFICIENCY BASED) REGRESSION	32
FIGURE 7.10. COMPARISON OF PREDICTED VERSUS MEASURED NO _x WITH TRAPPED EQUIVALENCE RATIO (IDEAL GAS BASED) REGRESSION.....	33

1. INTRODUCTION

This document provides a mid-term update for the “Advanced Compressor Engine Controls to Enhance Operation, Reliability, and Integrity” project. SwRI is conducting this project for DOE in conjunction with Cooper Energy Services, under DOE contract number DE-FC26-03NT41859. This report addresses the current status of engine controls for integral compressor engines and how they compare among each other.

2. OBJECTIVE

The objective of this one-year project is to develop, evaluate, and demonstrate advanced engine control technologies and hardware, specifically, closed-loop NO_x emissions control on a two-stroke integral reciprocating engine/compressor used for pipeline gas transmission service. This work will use a Cooper-Bessemer GMVH-6 laboratory engine owned by CES installed in a test facility at SwRI. The approach will involve three research activities including engine/test cell configuration, engine testing, and data analysis.

3. BACKGROUND

The gas transmission industry operates over 4,000 integral engine compressors, the majority being two-stroke, with a median age of 45 years and a median size of 2000 horsepower. These engines pump at least half of the 23 TCF of natural gas presently consumed in the United States. These engines are no longer produced, and with the projections for future increased demand of natural gas and the expense of replacement, it would be advantageous to modernize the existing fleet to allow for continued operation with increased efficiency and emissions compliance.

Integral gas compression engines have historically exhibited poor performance and high emissions, due in part to poor engine control. The end results are misfires and partial burns that lead to increased fuel usage and exhaust emissions. Many of the slow-speed integral engines in the gas compression industry utilize control systems that are outdated, slow, and suffer from poor resolution. The automotive and heavy-duty truck industries have advanced the state of electronics, sensors, and control algorithms for maximum efficiency, minimum emissions, and broadest operating envelope. Communications between the various power train components have also been developed for optimized operation and interaction between auxiliary systems.

To comply with future emissions legislation, and to increase industry wide competitiveness, existing engines need modern control systems and modern electronic sensors to maximize fuel economy while remaining emissions compliant. In addition, engine health monitoring and safety requirements mandate that additional sensors be installed to prevent inefficient operation, to be emission compliant, be pro-active in maintenance scheduling, expand the operating envelope, and allow for efficient operation at conditions that do not affect the structural integrity of the unit. The work reported in this document is a step toward bringing integral gas compression engine control and health-monitoring up to par with modern engine control technology, with new concepts that address the specific nature of integral compressor engine operation. The results of this program should compliment other industry funded programs for development of more sophisticated electronic engine controls.

4. TWO-STROKE INTEGRAL COMPRESSOR ENGINES

These engines are unique in that the compressor is integrated into the engine design, and is therefore not a separate component. A cross-sectional view of a typical integral compressor engine is provided in Figure 4.1. The compressors are reciprocating units, mostly double acting, with *pockets* to change the individual clearance volumes and, in-turn, the throughput of the individual compressors. The reciprocating design of the compressors creates an uneven loading on the engine within each revolution, and the sequence in which the pockets are opened or closed (load steps) creates an additional variance in the dynamic loading. Since the compressors are connected directly to the crankshaft, and a variable dynamic load is induced, the instantaneous rotational velocity (IRV) of the crankshaft is affected. Add in the fact that combustion is never completely stable, the IRV is further exacerbated.

The two-stroke integral engines are mostly loop scavenged with inlet and exhaust ports fixed in the cylinder liner. Port opening and closing is governed by piston motion. A few of the two-stroke engines are uniflow scavenged, which have inlet ports and exhaust valves. In both designs, the dynamic port timing is a function of the dynamic piston motion, or crankshaft IRV. During port/valve opening, the flow through the cylinder is governed by fluid dynamics, specifically the ratio of exhaust pressure to inlet pressure. Pulsations in the manifolds, due to design and/or unsteady combustion, affect the dynamic pressures during scavenging and create deviations in flow between cycles and cylinders. All the factors that affect airflow and cylinder scavenging, in turn affect the trapped air/fuel ratio and combustion.

An additional aspect of integral compressors engines, especially the two-stroke designs, is that they feature direct in-cylinder fuel admission to prevent scavenging of raw fuel into the exhaust. This direct fuel admission is performed with a cam-actuated poppet valve that has a fixed duration tied to crankshaft speed. The control variables with this design are the main fuel header pressure and individual *pinch* valves to each cylinder that are manually adjustable. A governor typically modulates the main fuel header pressure to maintain the engine speed setpoint. The pinch valves are manually adjusted to provide some compensation to individual cylinders to balance combustion across the engine.

Many of the two-stroke integral engines are turbocharged, or have been retro-fitted with turbochargers. The turbocharger comprises an exhaust turbine coupled to an inlet compressor. Typically, a wastegate is installed upstream of the exhaust turbine to bypass exhaust gas when less inlet air flow is required for the operating condition. Since fuel flow is utilized to govern engine speed, the wastegate can be used for global control of the air/fuel ratio. The most common control strategy is to control the inlet air pressure (wastegate) as a function of fuel pressure. Present-day systems utilize programmable logic controllers (PLC) to perform this task, along with functions such as start-up, shut-down, and safety alarming. The control strategies often emulate the predecessor manual-pneumatic control systems, and operate in an *open-loop* mode.

Ignition systems are becoming more sophisticated for these engines, progressing from a magneto style to systems with microprocessors. The newer systems offer the ability to program ignition timing as a function of engine speed and/or inlet manifold pressure. These systems, however, are

typically independent from the air/fuel controller with little or no communication. A schematic of a typical control system layout is provided in Figure 4.2.

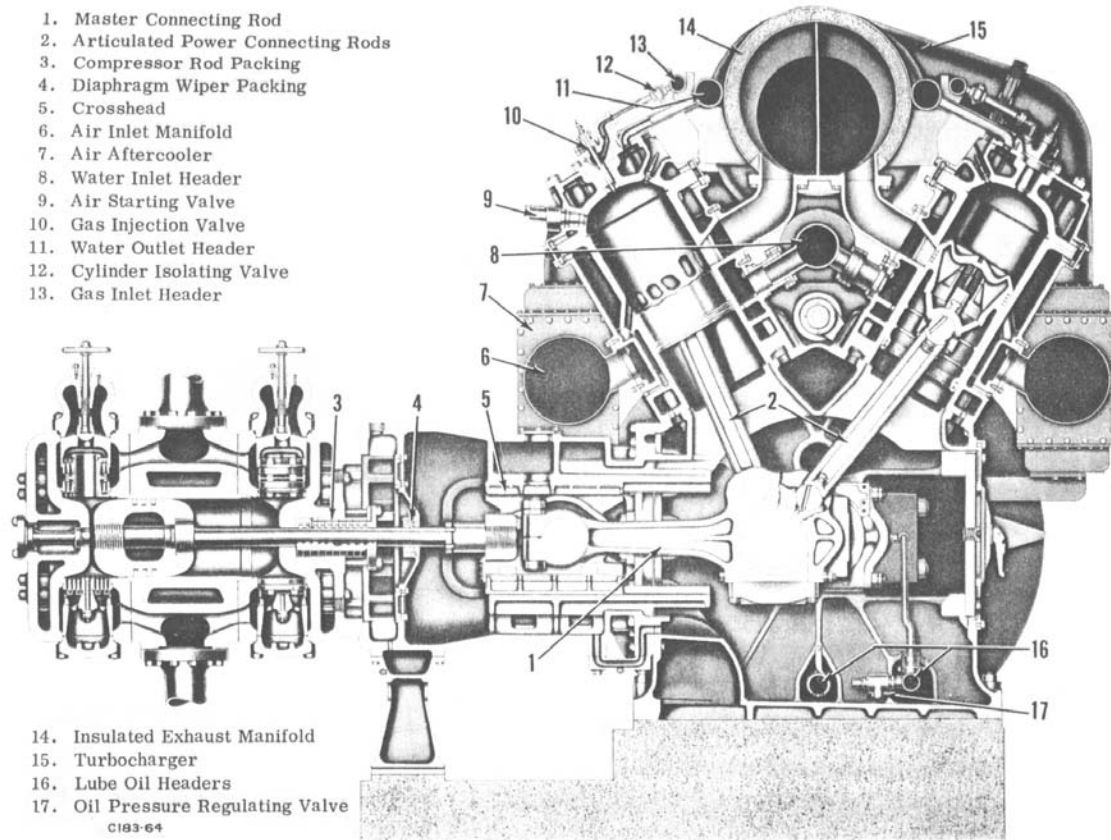


Figure 4.1. Cross Section of a Cooper-Bessemer GMVH Integral Compressor Engine

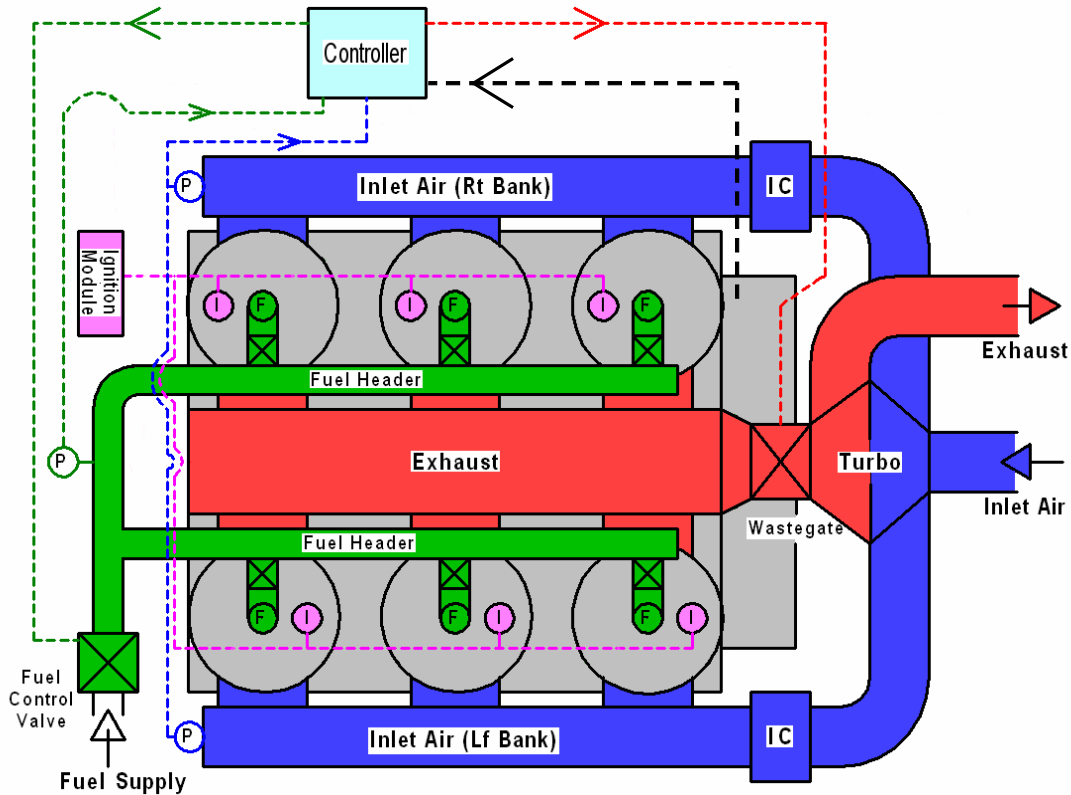


Figure 4.2. Typical Integral Compressor Engine Control System Layout

5. ENGINE CONTROL FUNDAMENTALS

5.1 Control Categories

The purpose of a control system is to maintain a desired process condition or output by regulating or adjusting parameters which the process is dependant. There are three main categories of control systems, though each category is comprised of an ever-evolving population of stratagems. The categories include manual control, open-loop control, and closed loop control.

- A manually controlled system is self-explanatory, wherein continuous operator involvement is necessary to maintain control.
- With open-loop control, the process inputs, $A(s)$, have no dependence on the process outputs, $C(s)$. Open-loop control schemes are often augmented with predictive algorithms based on a variety of measured or modeled parameters, $G_a(s)$. This often enable a more precise approximation of the output parameter, but the resulting “state” of the process output is not measured and/or not fed back to the control system.

- Closed-loop control requires feedback. The feedback is used to adjust or trim the open-loop scheme and command to the process, $F(s)$. The variety and complexity of closed-loop control systems stem from the algorithms implemented to determine the command, $G_a(s)$.

There are many techniques used to characterize the process under control, which helps to expedite controller design and meet the desired performance specification (i.e. stability, accuracy, and speed of response). Figure 5.1 depicts a common closed-loop control format including system elements and signals [1].

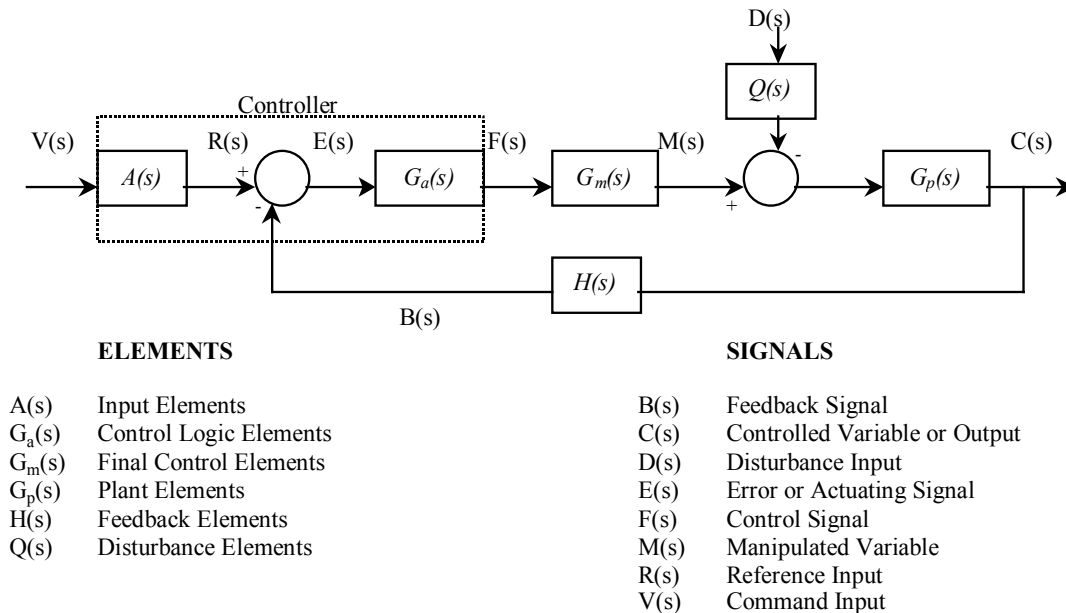


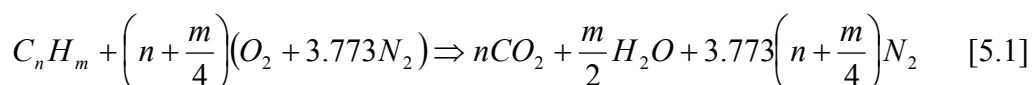
Figure 5.1. Terminology and Basic Structure of a Feedback Control System [1]

Controls for internal combustion engines are very widely depending on the type and application of the engine. The most advanced systems are used in automotive gasoline engines which are the greatest in number and therefore have the greatest impact on the environment – air pollution and energy consumption. As concerns for environmental impact of other engine types increases, electronic control systems for these engines increase in complexity. However, many of the systems for compressor engines are of the open-loop style, so there is much to be gained with closed loop control.

Closed-loop control for internal combustion engines has primarily focused on the use of air/fuel ratio feedback due to this parameter's significant impact on engine exhaust emissions and fuel consumption. Air/fuel ratio feedback is often in terms of fuel/air equivalence ratio, which is discussed in detail in the next section. Other closed-loop feedback signals can be utilized, such as NO_x emissions, depending on the control scheme and available sensors.

5.2 Fuel/Air Equivalence Ratio

Engine power, efficiency, and emissions are largely a function of the fuel-air mixture introduced into the engine. The ratio of fuel to air, or air/fuel ratio, is an important control parameter for spark-ignited engines which is optimized for performance and emissions. For each fuel composition, there is a specific mixture ratio where a hydrocarbon fuel can be completely oxidized called the stoichiometric air/fuel ratio. Complete oxidation at the stoichiometric ratio will cause the fuel carbon to be converted to carbon dioxide (CO₂) and the fuel hydrogen to be converted to water (H₂O). The chemical equation for complete oxidation of a hydrocarbon fuel is provided below:



Note the n and m terms in the hydrocarbon fuel symbol represent the moles of each element in the fuel. Since there are many different hydrocarbon fuels, with different molar proportions, it is common practice to utilize the hydrogen/carbon ratio of the fuel in the symbol as follows:



The equation for determining the stoichiometric air/fuel ratio on a mass basis for a hydrocarbon fuel then becomes [2]:

$$\left(\frac{M_{air}}{M_{fuel}}\right)_s = \frac{(1 + x/4)(32 + 3.773 \times 28.16)}{12.011 + 1.008x} \quad [5.3]$$

Some fuels, such as natural gas, also contain oxygen (in the form of CO₂) and nitrogen. The oxygen/carbon (y) and nitrogen/carbon (z) molar ratios are therefore required in addition to the hydrogen/carbon ratio (x) for determining the stoichiometric air/fuel ratio as follows [3]:

$$\left(\frac{M_{air}}{M_{fuel}}\right)_s = \frac{4.3211[15.999(2 + 0.5x - y + z)]}{12.011 + 1.008x + 15.999y + 14.007z} \quad [5.4]$$

Natural gas is a mixture of several constituents, and the molar percentages of each constituent must be known to calculate the stoichiometric air/fuel ratio accurately. The molar percentages of each constituent are also required to determine the overall fuel heating value. A gas chromatograph is typically employed to perform this measurement. An example measurement of natural gas composition, and the resulting calculations of stoichiometric air/fuel ratio, is provided in Table 5.1.

TABLE 5.1. EXAMPLE NATURAL GAS COMPOSITION AND STOICHIOMETRIC A/F RATIO

GC Mole Percent	Name	Formula	Molecular Weight	Lower HV BTU/lb	Mass Fraction
0.620	NITROGEN	N ₂	28.013	0	0.010
95.119	METHANE	CH ₄	16.043	21495	0.893
1.439	CARBON DIOXIDE	CO ₂	44.010	0	0.037
0.000	ETHYLENE	C ₂ H ₄	28.054	20275	0.000
2.095	ETHANE	C ₂ H ₆	30.070	20418	0.037
0.000	HYDROGEN SULFIDE	H ₂ S	34.082	6537	0.000
0.418	PROPANE	C ₃ H ₈	44.097	19937	0.011
0.079	ISO-BUTANE		58.123	19628	0.003
0.088	BUTANE	C ₄ H ₁₀	58.123	19678	0.003
0.041	ISO-PENTANE		72.150	19459	0.002
0.027	PENTANE	C ₅ H ₁₂	72.150	19507	0.001
0.042	HEXANE	C ₆ H ₁₄	86.177	19415	0.002
0.028	HEPTANE	C ₇ H ₁₆	100.204	19329	0.002
0.004	OCTANE	C ₈ H ₁₈	114.231	19291	0.000
0.000	OXYGEN	O ₂	31.999	0	0.000
0.000	HYDROGEN	H ₂	2.016	51623	0.000
0.000	PROPYLENE	C ₃ H ₆	42.081	19687	0.000
0.000	CARBON MONOXIDE	CO	28.010	4347	0.000
A/F Stoich		H/C Ratio	O/C Ratio	N/C Ratio	Lower HV BTU/lb
16.34		3.86	0.03	0.01	20399

Many spark-ignited engines, especially large-bore stationary, do not operate at stoichiometric air/fuel ratios. These engines often operate with excess air in a *lean-burn* configuration with actual air/fuel ratios much greater than stoichiometry. The many different fuel types, having different stoichiometric air/fuel ratios, and the different operating air/fuel ratios introduce complexity in control and comparison of performance among different engines. A more informative air-fuel parameter that normalizes these differences is the *fuel/air equivalence ratio* (Φ). The equivalence ratio is the ratio of the stoichiometric air/fuel ratio to the actual air/fuel ratio, as shown in the equation below. A value of unity for the equivalence ratio means stoichiometry, and values less than unity indicate lean operation. The inverse of the equivalence ratio, *lambda* (λ), is also sometimes used for a normalized air-fuel parameter.

$$\Phi = \lambda^{-1} = \frac{(A/F)_{stoich}}{(A/F)_{actual}} \quad [5.5]$$

As mentioned previously, the fuel-air equivalence ratio has a significant impact on engine exhaust emissions and fuel consumption. For lean-burn stationary engines operating at steady speed and load, there is an operating envelope bound by knock, misfire, and mechanical design

limits of peak cylinder pressure and pre-turbine temperature. This operating envelope is illustrated in Figure 5.2. The envelope as shown depicts the ignition timing versus fuel/air equivalence ratio. Within the bounds of the envelope, there is region of peak fuel efficiency for lines of constant NO_x emissions. Thus, the optimum operating point is a given spark timing and fuel/air equivalence combustion ratio that resides on the target NO_x emissions line and is located as close to the peak efficiency region as possible, with acceptable margins for misfire, knock, and mechanical limits.

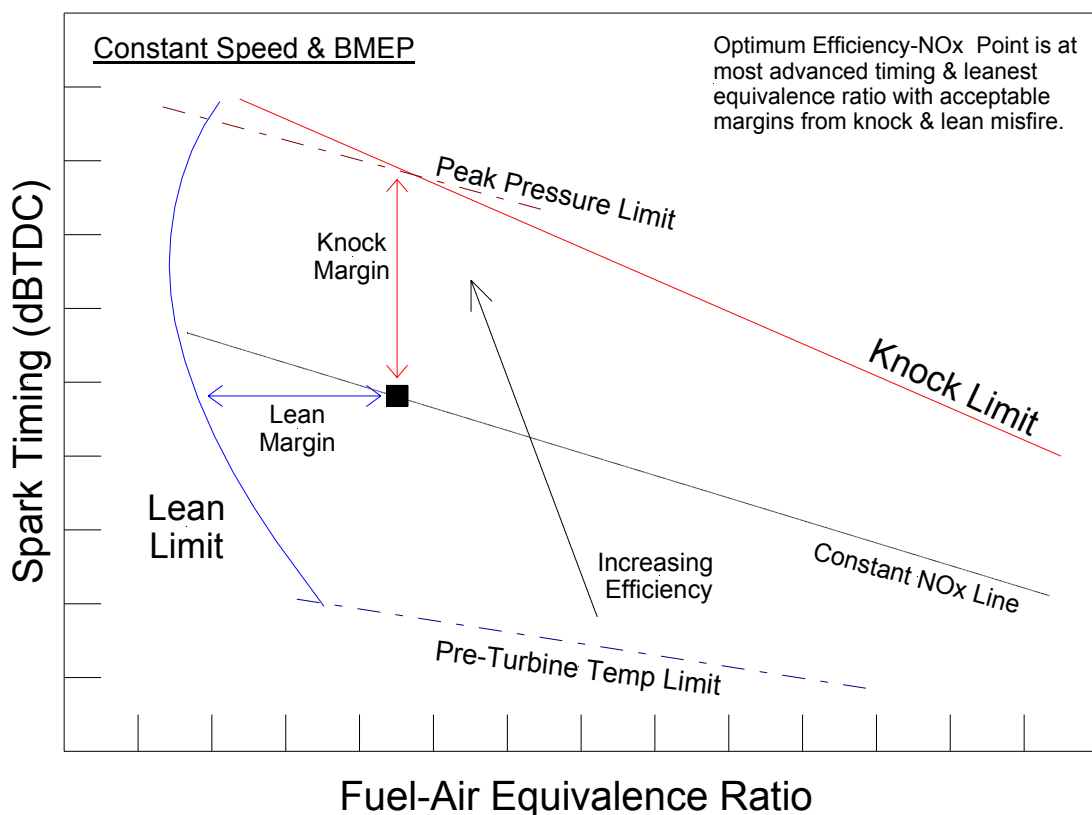


Figure 5.2. Typical Spark-Ignited Lean-Burn Operating Limit for Steady Speed & Load

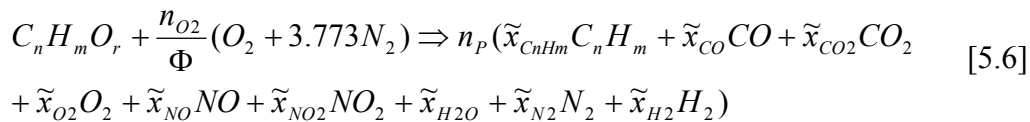
Determining the actual air/fuel ratio requires that the air and fuel flows both be accurately measured during operation. Smaller on-highway engines often utilize a hot-wire anemometer mass airflow sensor and an accurate calibration of the mass fuel flow versus injector pulse-width. In many instances with large-bore engines, one or both of these measurements is not readily available. Fuel flow is sometimes measured, but often the measuring device does not possess the accuracy or response required for real-time control. Many large-bore engines also do not utilize electronic fuel injection so fuel flow cannot be determined from an injector calibration. Fluid dynamic models may be used for fuel and air flows in large bore stationary engines, which operate primarily at steady-state conditions, with acceptable results if the inputs and coefficients are available and accurate.

An alternative approach is to measure the equivalence ratio directly with an exhaust gas oxygen (EGO) sensor. This is very common approach for on-highway engines. Automotive gasoline engine controls utilize an EGO sensor that switches in voltage output around stoichiometry, and

is used to trim the fuel flows. For lean-burn engines, a wide-range universal exhaust gas oxygen (UEGO) sensor can be utilized to control to a specific equivalence ratio. The UEGO sensor signal is calibrated for a specific fuel type, and gives an output directly proportional to equivalence ratio. The NGK-Locke NO_x sensor, described in Section 5.5, has the UEGO function as well as output for exhaust NO_x concentration. The EGO & UEGO sensors should be used in conjunction with measured or derived equivalence ratio in a feedback control loop, and to also provide redundancy and health monitoring.

5.2.1 Equivalence Ratio from Emissions

An accurate determination of fuel/air equivalence ratio can be derived from measurements of exhaust gas constituents. This method is ideal for laboratory engine testing and development, but is not practical for field engines and control due to the expensive and high maintenance analyzers required. However, this method is often utilized to calibrate engine performance, calculate equivalence ratio, and calibrate UEGO sensors for either engine development or tuning. A technique published by Heywood outlines the equivalence ratio determination from measurements of exhaust CO₂, CO, O₂, HC, and NO_x. The HC is assumed to be unburned fuel of the same properties as the supplied fuel. Any nitrogen in the fuel is typically very small, as shown in Table 5.1 above for natural gas, and therefore neglected. The modified chemical equation for incomplete combustion utilizing equivalence ratio and exhaust constituents is as follows [2]:



where:

$$n_{O_2} = \left(n + \frac{m}{4} - \frac{r}{2} \right) \quad [5.7]$$

$n_p =$ Total Moles of Exhaust

$\tilde{x}_i =$ Mole Fraction of *i*th Constituent

In many circumstances the measurements of CO₂, CO, O₂, and NO_x are performed from a dried exhaust sample by utilizing ice bath chillers. The HC measurement is typically from a fully wet sample with a flame ionization detector (FID). Given these types of wet/dry measurements, the calculation for equivalence ratio is as follows [2]:

$$\Phi = \frac{2n_{O_2}}{n_p \tilde{x}_{H_2O} + n_p (1 - \tilde{x}_{H_2O}) (\tilde{x}'_{CO} + 2\tilde{x}'_{CO_2} + 2\tilde{x}'_{O_2} + \tilde{x}'_{NO} + 2\tilde{x}'_{NO_2}) - r} \quad [5.8]$$

where:

$$\tilde{x}'_i(dry) = \frac{\tilde{x}_i(wet)}{(1 - \tilde{x}_{H_2O})} = \text{dry to wet relationship} \quad [5.9]$$

$$\tilde{x}_{H_2O} = \frac{m}{2n} \left(\frac{\tilde{x}'_{CO} + \tilde{x}'_{CO_2}}{1 + (\tilde{x}'_{CO} / K\tilde{x}'_{CO_2}) + (m/2n)(\tilde{x}'_{CO} + \tilde{x}'_{CO_2})} \right) \quad K \approx 3.5 \quad [5.10]$$

$$n_p = \frac{n}{\tilde{x}_{HC} + (1 - \tilde{x}_{H_2O})(\tilde{x}'_{CO} + \tilde{x}'_{CO_2})} \quad [5.11]$$

$$\tilde{x}_{H_2} = \frac{\tilde{x}_{H_2O}\tilde{x}'_{CO}}{K\tilde{x}'_{CO_2}} \quad [5.12]$$

$$\tilde{x}_{N_2} = \frac{3.773n_{O_2}}{\Phi n_p} - (1 - \tilde{x}_{H_2O}) \frac{(\tilde{x}'_{NO} + \tilde{x}'_{NO_2})}{2} \quad [5.13]$$

5.3 Two-Stroke Engine Equivalence Ratio

If the subject engine is a two-stroke spark-ignited engine, the equivalence ratio calculated from overall mass flows, UEGO sensor output, or exhaust measurements is the exhaust or *global* equivalence ratio. The value derived will be significantly leaner than the actual equivalence ratio for combustion, due to dilution of the exhaust gas with excess air that passes through the cylinder during scavenging. The actual equivalence ratio for combustion includes only the air mass trapped in the cylinder after the scavenging process is complete. This is therefore termed the *trapped equivalence ratio*, and the equation is as follows:

$$\Phi_{trapped} = \frac{(A/F)_{stoich}}{(A_{trapped}/F)_{actual}} \quad [5.14]$$

The equation above assumes that all the fuel admitted into the cylinder is trapped, which for direct in-cylinder admission/injection is a valid assumption. Trapped air mass is almost impossible to measure, except in tightly controlled laboratory environments with specialized instrumentation. Therefore, various techniques are utilized to estimate the trapped air mass for determining the trapped equivalence ratio.

5.3.1 Trapping Efficiency Technique

One technique for determining the trapped air mass is utilizing a technique outlined by Taylor. With this technique, the total mass airflow through the engine must be known (measured or modeled). A scavenging ratio is first determined as the ratio of the actual to the ideal mass air, typically in terms of a flow rate. The ideal air mass is that which would fill the cylinder at bottom dead center, or the maximum total cylinder volume. The equations for scavenging ratio are as follows [4]:

$$R_s = \frac{(\dot{M}_{air})_{actual}}{(\dot{M}_{air})_{ideal}} = \frac{(\dot{M}_{air})_{actual}}{N \cdot V_{cyl} \cdot \rho_s} \quad [5.15]$$

where:

\dot{M}_{air} = dry mass airflow

N = engine speed

V_{cyl} = total cylinder volume at bottom dead center

ρ_s = density of dry inlet air

$$= \frac{P_{exh}}{R_{air} \cdot T_{inlet}} \times \left(\frac{1}{1 + 1.6h} \right) \quad [5.16]$$

P_{exh} = pressure of trapped air, typically at exhaust pressure

T_{inlet} = temperature of trapped air, typically assumed to be inlet temperature

R_{air} = gas constant for air, assuming fuel admitted directly in-cylinder

h = mass fraction of water vapor in inlet air

With the scavenging ratio known, the scavenging efficiency can be calculated. The scavenging efficiency is the ratio of the air mass retained to the ideal mass retained. For the ideal case, the scavenging efficiency would equal the scavenging ratio, and is termed *perfect scavenging*. The opposite extreme case is termed *complete short-circuiting*, which is a process where the cylinder contents from the previous cycle are not scavenged exhausted and the fresh air flows straight through the cylinder from inlet to exhaust. In reality, two-stroke scavenging will be somewhere in between these cases with some air scavenging the residual, some air short-circuiting, and some of the fresh air charge mixing with the residual gas.

The most commonly assumed case for real operation is termed *complete mixing*, and assumes the fresh charge mixes completely with the residual gas. The scavenging and trapping efficiency equations for the complete mixing case are as follows [4]:

$$e_s = 1 - \exp^{-R_s} \quad \text{scavenging efficiency} \quad [5.17]$$

$$\Gamma = \frac{e_s}{R_s} = \frac{1 - \exp^{-R_s}}{R_s} \quad \text{trapping efficiency} \quad [5.18]$$

The accuracy of the complete mixing case depends on several factors, including the scavenging arrangement (loop, cross, uniflow, etc.), the mean piston speed (or engine speed), and inlet to

exhaust port/valve geometry differences. Published data from detailed laboratory experiments of scavenging in two-stroke engines of various sizes and types have shown a deviation from the complete mixing case with changing mean piston speed [2, 4]. Therefore, a possible correction procedure can be determined, provided data for a given engine exists to properly derive the magnitude and function, to account for speed dependencies. The correction could be an offset for the scavenging type (engine specific) and a multiplier for operating condition affects (i.e. engine speed). The resulting equation could be in the following form:

$$(e_s)_{corr} = ((1 - \exp^{R_s}) + A) \times B \quad [5.19]$$

Once the trapping efficiency has been estimated, the trapped mass airflow can be computed and used to calculate the trapped equivalence ratio. The trapped mass airflow is simply the total mass airflow times the trapping efficiency. The resulting equation for trapped equivalence ratio using trapping efficiency is as follows:

$$\Phi_{trapped} = \frac{(A/F)_{stoich}}{\frac{\Gamma(\dot{M}_{air})_{total}}{\dot{M}_{fuel}}} \quad [5.20]$$

The total mass airflow through the engine can be measured, or predicted from either empirical based models or with fluid flow based models. One technique for predicting the mass airflow is the utilization of equations outlined by Taylor for flow of gas through two orifices in series. The inlet and exhaust ports/valves act as orifices, with the cylinder as the volume separating the orifices. This method derives a continuous mass flow, representative of the total mass airflow, which can be used directly in the equivalence ratio equation above with the measured fuel mass flow. The mass airflow equation is as follows [4]:

$$\dot{M}_{air} = ACa\rho\phi_1 \quad [5.21]$$

where:

$A =$ orifice area, or reference area (piston bore area is a convenient reference)

$C =$ orifice flow coefficient (ratio of actual mass flow to ideal flow through reference area under similar conditions)

$a =$ speed of sound in gas in upstream reservoir

$\rho =$ density (typically derived at inlet temperature and exhaust pressure)

$$\phi_1 = \sqrt{\frac{2}{\gamma - 1} \left[\left(\frac{P_{exh}}{P_{int}} \right)^{\frac{2}{\gamma}} - \left(\frac{P_{exh}}{P_{int}} \right)^{\frac{\gamma+1}{\gamma}} \right]} \quad [5.22]$$

non-choked flow - for air, when $\gamma=1.4$, $\left(\frac{P_{exh}}{P_{int}}\right) > 0.528$

$$= \sqrt{\left(\frac{2}{\gamma+1}\right)^{\frac{\gamma+1}{\gamma-1}}} \quad [5.23]$$

choked flow - for air, when $\gamma=1.4$, $\left(\frac{P_{exh}}{P_{int}}\right) \leq 0.528$ ($\phi_l = 0.578$)

The key to accurate estimation of mass airflow with this technique is the proper determination of the flow coefficient value. For most two-stroke engines under firing conditions and typical pressure ratios of 0.65 to 0.95, the flow coefficient will range from 0.02 to 0.035. While the flow coefficient is primarily a function of the pressure ratio across the cylinder, the engine speed and combustion profile will affect it slightly.

The scavenging process occurs over only a portion of the cycle, and the airflow is therefore non-steady. Engine speed affects the time duration of the scavenging process, which in turn affects the instantaneous airflow, but is offset somewhat by the change in number of events per unit time. The combustion process can affect the cylinder pressure at time of port/valve opening, and therefore instantaneous airflow, depending on the firing pressure and phasing of combustion (early or late). Parameters such as ignition timing and the trapped equivalence ratio affect the combustion profile. Since the trapped equivalence ratio is the focus of this derivation, then easily measured surrogate parameters such as fuel mass or pressure could be used to indicate relative changes in air/fuel ratio and combustion affects on the actual airflow from this technique.

5.3.2 Ideal Gas Law Technique

A technique to estimate the trapped air mass directly is to utilize the ideal gas law. The ideal gas law equation is rearranged to solve for mass with pressure, volume, temperature, and gas properties as inputs. This method is somewhat similar to the calculation of the ideal total mass flow for the denominator in the scavenging ratio calculation above, except that this method is for the ideal trapped mass airflow. The pressure is assumed to be the exhaust pressure near port/valve closure, due to the fact exhaust ports/valves typically close after the inlet. It is assumed that the cylinder pressure is very near exhaust pressure at the beginning of compression. The volume is assumed to be the total cylinder volume at the period of exhaust port closing where inflow/outflow has ceased. The temperature is often assumed to be similar to the inlet air temperature, but in actuality is likely higher due to heat transfer from the combustion chamber walls during scavenging. A simple method to partially account for this phenomena is to calculate a weighted average of the inlet air and jacket wall temperatures [5]. Finally, the gas properties are assumed to be for air. This technique also assumes that displacement of air mass in the cylinder by fuel mass is negligible. Equations for ideal gas based trapped mass airflow are as follows:

$$(m_{air})_{trap} = \frac{P_{exh} V_{trap}}{R_{air} T_{inlet}} \quad [5.24]$$

$$(\dot{M}_{air})_{trap} = (m_{air})_{trap} \times N \quad [5.25]$$

This method may be slightly more susceptible to engine speed and combustion profile affects than the flow coefficient based fluid dynamic model. Fletcher et al outlined the correlation of NO_x emissions with trapped equivalence ratio for an approach similar to this technique, and showed a greater engine speed correction is required than with the trapping efficiency based technique [5].

5.4 NO_x Emissions

NO_x refers to the mixture of nitric oxide (NO) and nitrogen dioxide (NO₂). Typically, over 90 percent of the NO_x formed during combustion is NO, but some of the NO will oxidize to NO₂ as it cools during expansion or in the exhaust (and in the sample line to the analyzer). Additional oxidation of NO to NO₂ can occur in the environment, and it is the NO₂ that reacts to form photo-chemical smog. NO_x is typically assigned the molar mass of NO₂ since all the NO can ultimately be oxidized to NO₂ [6].

The formation of NO_x is complex and strongly dependent on flame temperature. Flame temperature is highest just rich of stoichiometric, but since formation of NO_x also requires oxygen, the peak production will be slightly lean of stoichiometry. This is illustrated in Figure 5.3, published by Heywood [2]. The time period at critical flame temperature also influences NO_x formation. Therefore, low flame speeds with lean mixtures, or reduced engine speed, provide a longer period of time for NO_x to form.

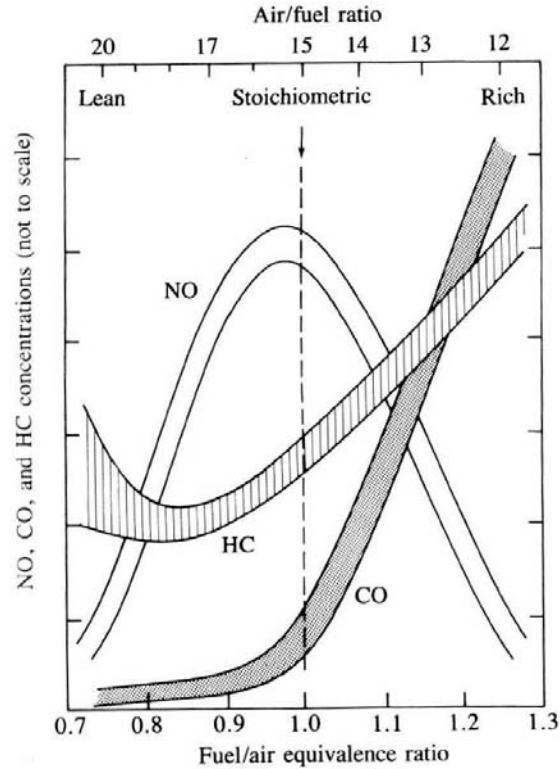


Figure 5.3. Exhaust Emissions Versus Equivalence Ratio [2]

NO is formed during combustion by three mechanisms: thermal, prompt, and nitrous oxide [6]. The extended Zeldovich mechanism provides the basis for the thermal mechanism. The rate equation and the three reaction equations are given below. Rate coefficients from two sources for each reaction are given in Table 5.2.

$$k_i = A_i \times T^{\beta_i} \times \exp\left(-\left(\frac{E}{R_o}\right)_i T\right) \quad [5.26]$$

where:

k_i = reaction rate coefficient

T = temperature ($^{\circ}K$)

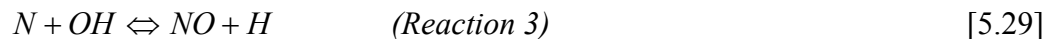
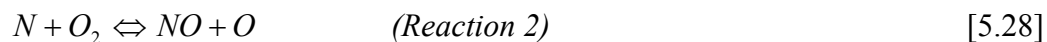
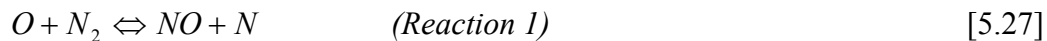
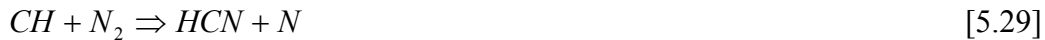


TABLE 5.2. RATE COEFFICIENTS FOR THE THERMAL NO MECHANISM

Source	Reaction 1			Reaction 2			Reaction 3		
	<i>A</i>	β	<i>E/R₀</i>	<i>A</i>	β	<i>E/R₀</i>	<i>A</i>	β	<i>E/R₀</i>
Heywood [hey]	1.6E+13	0.0	0.0	6.4E+9	1.0	3150	4.1E+13	0.0	0.0
Miller & Bowman [m&b]	3.3E+12	0.3	0.0	6.4E+9	1.0	3160	3.8E+13	0.0	0.0

The thermal mechanism rate constants are very slow compared to those for combustion. Therefore, the thermal NO mechanism is significant only when there is high enough flame temperature and sufficient time at temperature for formation. Measurements of NO concentration in the burnt gases do not extrapolate to zero at the flame, implying NO is formed in the flame by the prompt mechanism [6]. The prompt NO mechanism is significant when flame temperature is low enough to make the thermal mechanism negligible, or when there is fuel-bound nitrogen. The prompt mechanism is described by the following governing equation [6]:



The nitrous oxide mechanism is also only important at low temperature, and is governed by the following equation:



The nitrous oxide will decompose to NO, and this mechanism is significant with lean pre-mixed laminar flames [6].

In fuels for spark-ignition engines, the fuel-bound nitrogen is small and can be considered negligible for NO formation. The combustion temperature in internal combustion engines is high and the flame reaction zone thin with short residence time. Thus, the thermal mechanism is dominant. Therefore, NO (or NO_x) predictions are usually based on the extended Zeldovich mechanism. Combining the reaction equations above and rearranging results in the NO rate of formation equation below [2]:

$$\frac{d[NO]}{dt} = \frac{2R_1 \{1 - ([NO]/[NO]_e)^2\}}{1 + ([NO]/[NO]_e)R_1/(R_2 + R_3)} \quad [5.31]$$

where:

$$R_1 = k_1^+[O]_e[N_2]_e = k_1^-[NO]_e[N]_e$$

$$R_2 = k_2^+[N]_e[O_2]_e = k_2^-[NO]_e[O]_e$$

$$R_3 = k_3^+[N]_e[OH]_e = k_3^-[NO]_e[H]_e$$

[]_e = equilibrium concentration

The equation above is for use in complex chemical kinetic models. Simplification of the rate equation for purposes of data trending during engine development or for simple model-based controls have often been performed [7,8,9]. These simplifications typically ignore factors such as concentrations of N₂ and O₂, and time constants. One such simplified routine published by Wood is for predicting the relative change in NO_x, and requires a baseline or reference data for coefficient derivation [7]. This simple equation is as follows:

$$NO_x = B \times \exp\left(-\frac{A}{T}\right) \quad [5.32]$$

where:

$$\begin{aligned} A &= \text{constant (activation energy)} \\ B &= \text{constant (specific to application)} \\ T &= \text{peak combustion temperature} \end{aligned}$$

Modified for relative change from a reference condition:

$$\frac{NO_x}{(NO_x)_{ref}} = \exp\left[A \times \left\{ \left(\frac{1}{T}\right)_{ref} - \left(\frac{1}{T}\right) \right\}\right] \quad [5.33]$$

The peak combustion temperature can be calculated from thermodynamic analysis of measured cylinder pressure, and trapped masses of fuel, air, and residual. The peak combustion temperature can be substituted by the bulk gas temperature from ideal gas analysis or estimated temperature from ideal cycle equations. As long as the method is consistent, the coefficients can be fit for a given reference condition. The temperature equation presented by Wood is as follows [7]:

$$T = T_1 \times r^{(k-1)} + \frac{(HV \times m_{fuel})}{(C_V \times m_{total})} \quad [5.34]$$

where:

$$\begin{aligned} T_1 &= \text{temperature at start of compression} \\ r &= \text{effective compression ratio} \\ k &= \text{ratio of specific heats (typically 1.4 used)} \\ HV &= \text{fuel heating value by mass} \\ m_{fuel} &= \text{trapped mass of fuel} \\ m_{total} &= \text{trapped mass of fuel, air, and residual} \\ C_V &= \text{specific heat of cylinder gasses} \end{aligned}$$

Another use for a simplified NO_x rate equation is for parametric emissions monitoring (PEMS) and engine control. Beshouri published a PEMS approach utilizing an equation similar to 4.31 where both coefficients are tuned via empirical data [9]. Once the equation is tuned for a specific engine or model, and an acceptable error margin selected, the system can provide a continuous prediction of NO_x emissions for determining whether or not the engine is maintaining compliance. The temperature calculation used by Beshouri is an *effective bulk*

temperature (T_{eb}), which requires measurement of cylinder pressure, and is determined as follows [9]:

$$T_{eb} = \frac{P_p \cdot V_{eff}}{P_{fill} \cdot V_{fill}} \times T_{fill} \quad [5.35]$$

where:

T_{fill} = cylinder filling temperature (air manifold temperature)
 P_{fill} = cylinder filling pressure (air or exhaust manifold pressure)
 V_{fill} = trapped cylinder volume (at port/valve closure)
 V_{eff} = empirical effective volume
 P_p = peak cylinder firing pressure

5.5 NGK-Locke Combined NO_x/O₂ Sensor

Most of the methods and techniques discussed in Sections 5.2 through 5.4 can be utilized for use in electronic engine controls. To expand from open-loop type control algorithms to closed-loop strategies, a feedback signal is required. The sensor developed by NGK-Locke provides such a feedback. The NGK-Locke sensor combines the UEGO function with direct measurement of exhaust NO_x concentration. Therefore, one or both of these signals can be utilized as feedback to adjust or trim the fuel or airflow control signals.

The sensor is a solid-state, thick film, amperometric, electrolyte type containing multiple diffusion cells and a temperature controlled sensing element [10,11,12,13]. The output of this sensor is in the form of a 0-5 volt signal and compatible with present day engine control management (ECM) systems. The combined NO_x range of this sensor can be as high as 0-2000 parts per million (ppm) and has a published response time of 260 msec for a 33 to 66 percent step change in NO_x [11]. This sensor catalytically converts NO₂ to NO to determine total NO_x [12]. A photograph of the NGK-Locke sensor and electronic module is provided in Figure 5.4.

Calibration data for the NO_x signal and UEGO signal used on a GMVH-6 integral two-stroke engine are provided in Figures 5.5 and 5.6, respectively. For these calibrations, the NO_x was measured by a laboratory grade chemiluminescence analyzer and the exhaust equivalence ratio was determined from emissions measurements using equation 5.8. As seen in these plots, an exceptionally good calibration was derived, even in the high oxygen content and low temperature exhaust stream of a slow-speed two-stroke engine.

If the control logic is based on global equivalence ratio, the UEGO channel can be utilized for direct feedback to adjust the open-loop fuel calculation/calibration, while the NO_x signal can provide a limiting function. For a two-stroke engine where trapped equivalence ratio is the focus, it is envisioned that the global equivalence ratio feedback can be utilized to tune the trapped mass calculations for greater accuracy. If a NO_x prediction algorithm is employed, the NO_x signal can provide a direct feedback to tune the model. A discussion on control strategies is provided in the next section.



Figure 5.4. Photograph of NGK-Locke Combined NO_x/O₂ Sensor

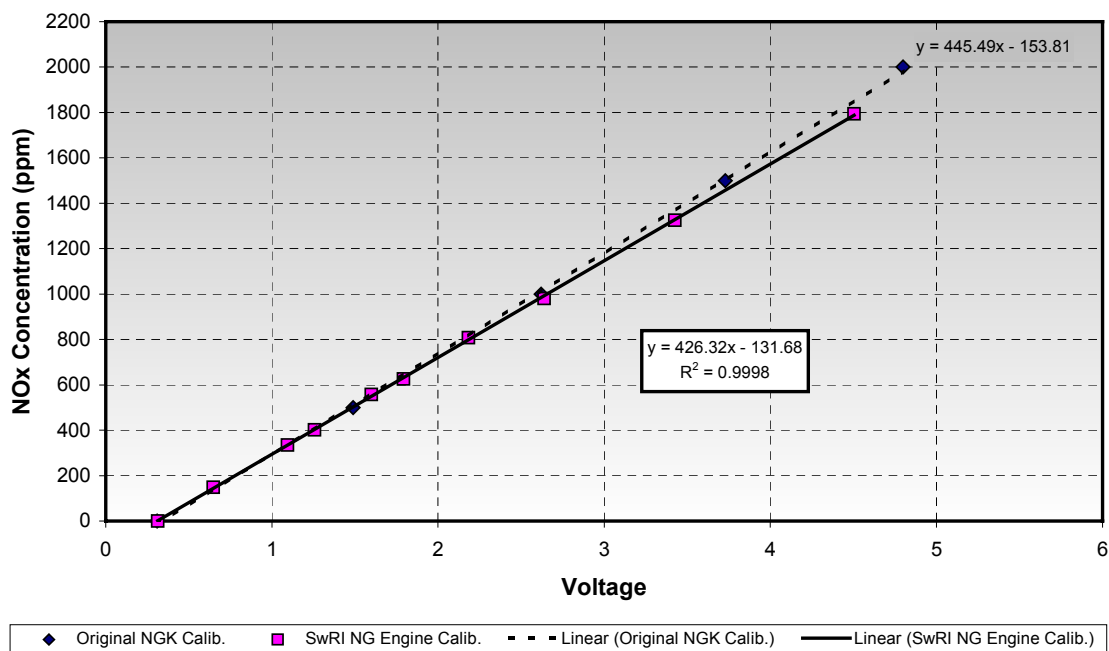


Figure 5.5. Calibration of NGK-Locke NO_x Signal on GMVH-6 Engine

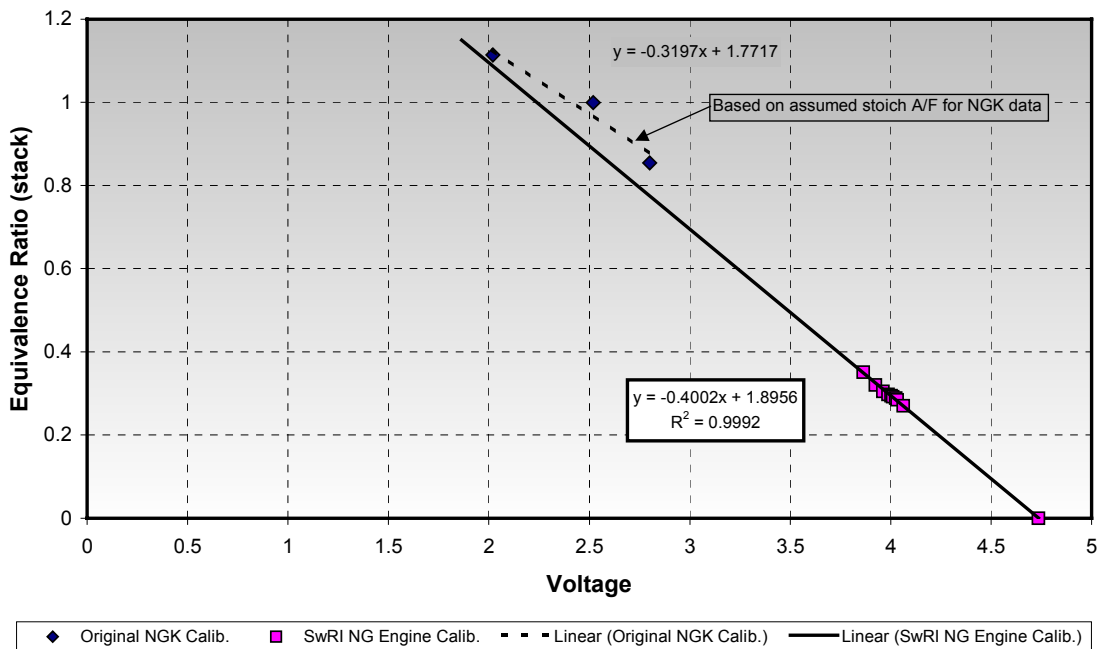


Figure 5.6. Calibration of NGK-Locke UEGO Signal on GMVH-6 Engine

6. COMPRESSOR ENGINE CONTROLS

Integral gas compression engines have historically exhibited poor performance and high emissions due in part to poor engine control. The end results are misfires and partial burns that lead to increased fuel consumption and exhaust emissions. Most existing control systems lack the technology, sensors, and algorithms to detect and correct for out-of-range sensors or mal-performance. Modern electronic controls are being developed and implemented that deal specifically with compliance to a specified emissions level. These modern control systems typically include empirically derived and model based relationships to predict NO_x emissions as a function of either estimated trapped equivalence ratio or as a direct result of engine operating parameters.

6.1 Fuel-Air Curve

The traditional approach for air/fuel control is to utilize a *fuel-air curve*. This curve is a linear relationship between the fuel header pressure (mechanical fuel admission valves) and air manifold pressure (inlet or boost pressure). This curve accounts for engine speed and load changes, where the air manifold pressure (AMP) is adjusted to maintain the relationship with fuel header pressure (FHP). FHP is a result of governor response to maintain the engine speed setpoint. Therefore, air follows fuel in this approach. Adjustments to account for affects of air manifold temperature (AMT) are provided by developing offsetting curves. Derivation of this curve is empirically based from calibrating the engine in the operating envelope. This is an open-loop strategy that does not ensure a specific air/fuel ratio setpoint is always maintained, nor

does it ensure that a NO_x emissions level is always maintained. An example of such a fuel-air curve was provided by Cooper Energy Services, and is depicted in Figure 6.1 below.

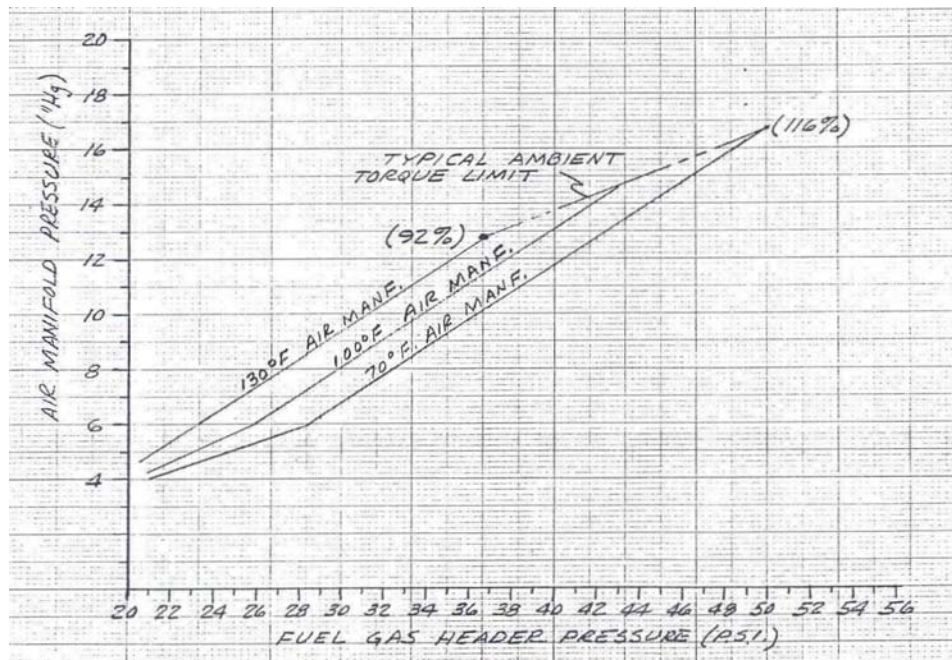


Figure 6.1. Example Fuel-Air Curve

6.2 Corrected AMP Setpoint

Another control strategy published by Matthews et al utilizes an AMP setpoint similar to the fuel-air curve above, except the AMP setpoint is a function of the desired equivalence ratio rather than FHP [14]. As can be seen in the equations in Section 5.3, there are several measured parameters required for the various derivations. Several of these parameters are not typical measurements currently performed on compressor engines today (i.e. exhaust pressure). Therefore, this method seeks to minimize required measurements and to derive a setpoint that would be familiar to station personnel that is familiar with the fuel-air curve.

The AMP setpoint method involves combining and re-arranging equations 5.14, 5.24, and 5.25 to solve for the AMP (inlet gage pressure) for a specific trapped equivalence ratio. The desire for a specified trapped equivalence ratio stems from the well documented relationship of NO_x emissions as a function of trapped equivalence ratio. Methods to compensate for engine speed dependency are addressed with a correction in the form of a polynomial equation. This method provides increased accuracy over the fuel-air curve in that trapped equivalence ratio, and therefore NO_x emissions, are addressed and controlled.

6.3 Trapped Equivalence Ratio

The fuel/air equivalence ratio is becoming more utilized as a control parameter in controls for integral gas compression engines [5,15,16]. Regulations for NO_x emissions have driven the need to develop control strategies that can maintain or limit the NO_x level emitted from engines

that must comply with these regulations. Since NO_x emissions are strongly a function of the fuel-air equivalence ratio, controlling the engine to operate at a specified equivalence ratio largely affects the engine-out NO_x emissions.

The implementation on two-stroke integral engines typically involves calculation of trapped equivalence ratio with equations 5.14, 5.24, and 5.25, and developing an empirically based relationship for NO_x emissions. Adjustment parameters such as engine speed, ignition timing, inlet temperature, and even engine type are implemented as correction factors to the calculated trapped equivalence ratio [5,15]. The objective is to reduce the multi-parameter regression to one relationship of NO_x versus corrected trapped equivalence ratio for all operating conditions and for all similar engines. With a large base of historical data behind the development of the regression model, minimum calibration data points should be required when commissioning this approach on a new unit.

6.4 Cylinder Pressure Based PEMS

Another advanced control strategy being developed for integral compressor engines is the use of models derived for PEMS systems. As described in Section 5.4, NO_x emissions can be predicted reasonably well with a simple equation based on the peak combustion, or effective bulk gas temperature. For control purposes, the model can be rearranged where instead of predicting NO_x for a given operating condition, the operating parameters can be determined for a given NO_x setpoint [9]. This method requires use of continuous cylinder pressure monitoring for the derivation of temperature with equation 5.35.

Development of low cost and durable continuous cylinder pressure transducers remains challenging, however progress is being made. Kistler has developed a piezo-electric transducer with integrated charge amplifier. IMES has developed a strain-gauge based transducer. Optrand and Fiber Dynamics have fiber optic transducers available. There is also interest in even lower cost sensors, such as load washers, that can provide indicating values peak pressure and location of peak pressure.

6.5 Integrated Engine-Compressor Controls

SwRI conducted a program for GMRC and PRCI to investigate the coupling of engine and compressor controls [17]. The premise for this research was that the compressor control and engine control should be coupled for optimal control of both. It was theorized that cyclical loading of the compressors could impart sufficient variations in crankshaft IRV where cylinder scavenging and combustion in various power cylinders could be affected, especially when loading between compressors was uneven. Data acquired during this project showed that NO_x emissions was affected by the compressor load step for a given engine speed and compressor horsepower. A follow-up program funded internally by SwRI also recorded similar effects on NO_x emissions. Additional research into this phenomenon is planned to determine the factors contributing to consistent step changes in NO_x with load step [18].

6.6 Enabling Technology

Other low-emissions technology for integral compressor engines is being developed. The interest in these technologies in terms of engine control is the potential for enabling more advanced strategies and algorithms. The technologies of interest are as follows:

- Electronic Fuel Injection (EFI) – EFI for integral compressor engines is currently available from Enginuity, Hoerbiger, and DigiCon. These systems involve elevated injection pressures from the standard mechanical poppet valve system. The higher pressures and nozzle designs are primarily for improved in-cylinder mixing to achieve more repeatable combustion. The advantage for electronic controls is the ability to control injection duration (speed governing), injection timing, and individual cylinder biasing as a function of engine operating conditions. An accurate calibration to enable real-time fuel flow per cylinder and per cycle could offer many benefits for optimizing the engine performance, providing better diagnostics, and enabling more sophisticated model-based control algorithms for individual cylinder control.
- Pre-Combustion Chambers (PCC) – PCC has been available for many years from Cooper Energy Services and several engines feature these as part of low-emissions retrofits. Dressor-Rand, CECO, and Diesel Supply, among others, also manufacture PCC's for compressor engines. The PCC offers tremendously increased ignition energy, that overcomes poor in-cylinder mixing and greatly improves combustion stability. With a PCC, combustion occurs in the small chamber, and the hot combustion gasses exiting the pre-chamber penetrate the main chamber. This process enables significantly leaner operation and, in turn, lowers NO_x emissions. The benefit is more repeatable combustion over a wider operating range for less stringent requirements on monitoring/calculating limits of operation. Additionally, measurements for control logic calculations will be more stable with the reduced combustion instability, providing potentially more accurate real-time control.
- Ionization Current Feedback – Ionization current results from the application of a positive DC voltage to the spark plug electrodes. The current signal profile provides indication of misfire, knock, and air/fuel ratio. The current signal is low, in the milliamp range, and becomes lower with leaner equivalence ratios. These systems are becoming more prevalent in automotive applications. Woodward Governor is developing a system for large-bore stationary engines. The benefits of such a system for controls are many. The signal can be used as a closed-loop control feedback for misfire detection, knock detection, and diagnostics. This system can potentially enable a more aggressive calibration, with reduced knock and misfire margins, for increased efficiency.
- Knock Detection – Knock detection is very common in automotive engines and control systems. Knock detection systems for large-bore spark-ignited engines are becoming available. Combustion knock, or detonation, results in a high frequency sound wave through the mechanical structure of the engine. This high-frequency *ringing* can be detected with accelerometer based sensors tuned to the knock frequency of a particular engine. A knock detection system enables a more advanced ignition timing, to be used for improved efficiency

while offering the ability to protect the engine from damage. When knock is detected, the control system can either retard timing or lean the air/fuel mixture.

7. RESULTS AND DISCUSSIONS

The GMVH-6 laboratory engine was tested in both open chamber and PCC configurations over a wide range of operating conditions. The operating parameters that were varied include the following:

- Engine Speed – from 330 to 198 rpm
- Engine Load – from 100 to 60 percent rated BMEP
- Spark Timing – from near knock limit to well retarded from optimal
- Air/Fuel Ratio – from lean limit, or closed wastegate, to near knock limit

Also included in the database are variations in ambient humidity. Trapped equivalence ratio control strategies are the most prevalent in current control systems being developed for integral compressor engines. Therefore, the data analysis was performed as follows:

- 1) Validation of measured total mass airflow
- 2) Comparison of predicted to measured total mass airflow
- 3) Analysis and comparison of estimated trapped mass airflow
- 4) Comparison of trapped equivalence ratio techniques
- 5) Comparison of predicted NO_x using equivalence ratio techniques

7.1 Mass Airflow and Trapped Air Mass

The first part of the analysis was to evaluate the techniques for total and trapped air mass derivation. The GMVH engine is fitted with an ASME nozzle in the inlet to measure volumetric airflow for all data points. For each data point, full emissions data and fuel gas composition was acquired. The stoichiometric air/fuel ratio was calculated from the fuel gas composition. The exhaust (global) equivalence ratio was calculated from emissions using equation 5.8. These values, plus measured fuel mass flow, were used to calculate the total mass airflow by rearranging equation 5.5. The mass airflow derived from emissions and fuel flow is a *dry* mass airflow. The measured mass airflow from the ASME nozzle is a *wet* mass airflow, which was corrected to a dry mass airflow with the measured ambient humidity. A comparison of the dry ASME nozzle airflow and mass airflow from emissions is depicted in Figure 7.1. As seen in this figure, a very good correlation exists between these values.

The total airflow model based on equation 5.21 was then compared to the total mass airflow. The total mass airflow from emissions and fuel flow were used as the basis of this comparison. Figure 7.2 depicts the comparison of the modeled total mass airflow. This figure illustrates that the model does a good job of predicting the total mass airflow, with an accuracy of approximately ± 5 percent.

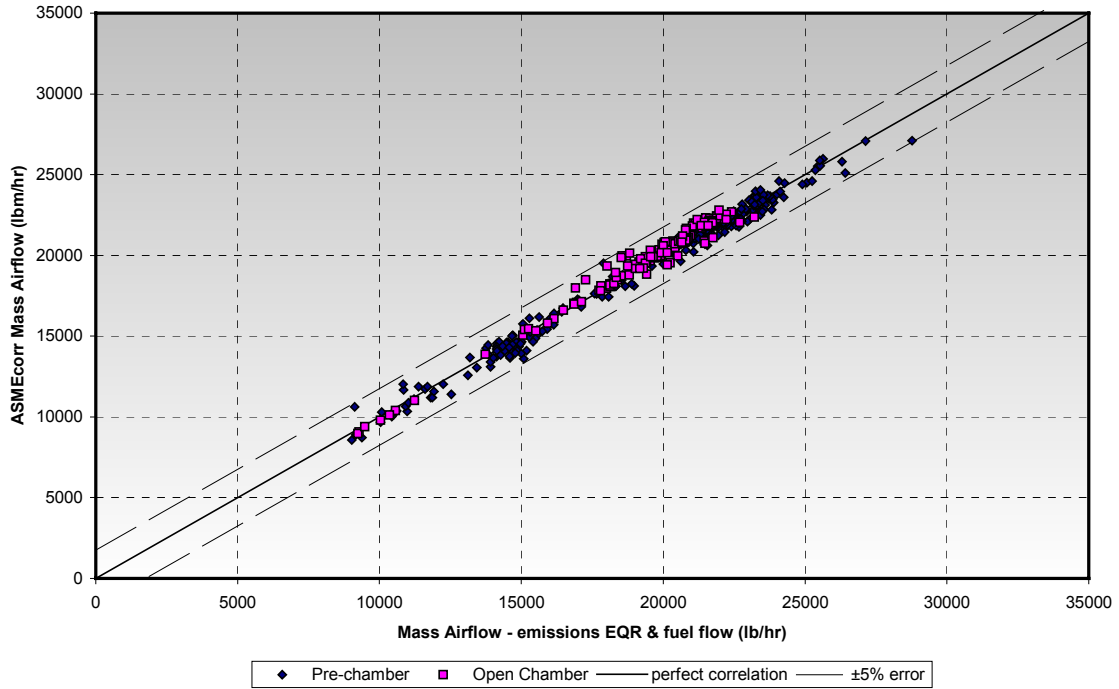


Figure 7.1. Comparison of Dry Total Mass Airflows from Emissions and ASME Nozzle Measurements

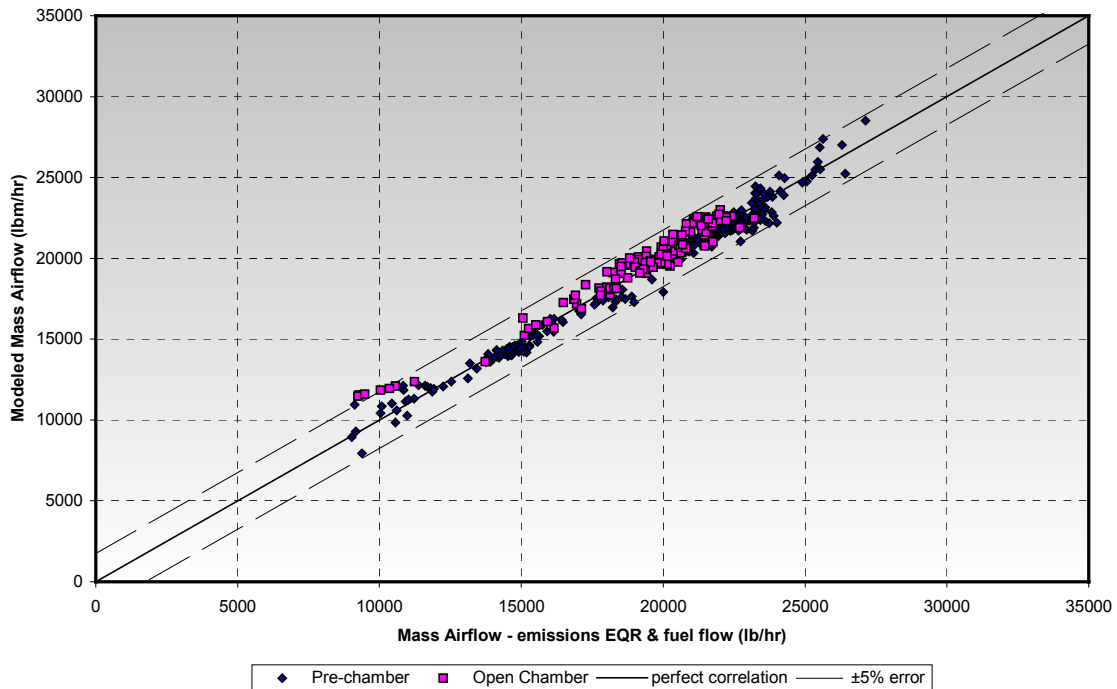


Figure 7.2. Comparison of Dry Total Mass Airflow from Emissions and Modeled Total Mass Airflow

As part of the modeled total mass airflow prediction, a flow coefficient is required as discussed in Section 5.3.1. To derive this coefficient, the calculation (equation 5.21) was rearranged to solve for the flow coefficient with the measured mass airflow utilized as input. The result was a non-linear function versus the pressure ratio. A sensitivity study was then conducted to determine the impact of various parameters. A function was derived that included the pressure ratio (by far the dominant parameter), engine speed, and fuel header pressure as a surrogate to the air/fuel ratio or combustion affect on flow. The model only includes the inlet and exit (orifice) pressures, and does not include the cylinder (volume) pressure. Depending on whether the combustion is early or late, the cylinder pressure at port opening can vary greatly and affect the velocity through the ports. Therefore, the air/fuel ratio was presumed to have a strong affect on the cylinder pressure at port opening and, in turn, the flow coefficient. Since the trapped air/fuel ratio is unknown at this point, fuel header pressure was utilized as the surrogate. A comparison of the flow coefficient back-calculated with measured airflow to the derived flow coefficient is depicted in Figure 7.3. The trend profile of this data was compared to data shown by Taylor [4] and, within the range of pressure ratios measured on the GMVH, compared well.

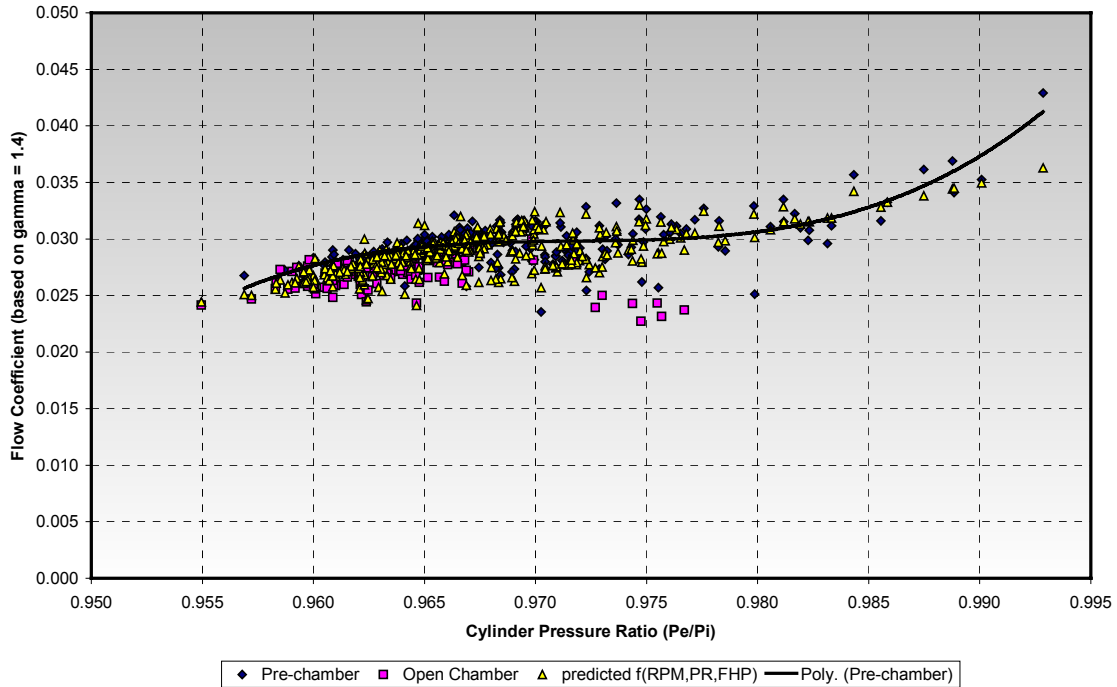


Figure 7.3. Comparison of Flow Coefficient Derived from Measured Airflow and Predicted from Regression Model

The next step was to calculate the trapped mass airflow. The two methods described in Section 5.3 were employed. For this analysis, the measured exhaust pressure and inlet temperature were utilized for estimating the trapped cylinder density. The trapping efficiency was based on the assumption of complete mixing (further investigation into the applicability of this assumption is planned). The measured mass airflow was used in the trapping efficiency based derivation, as it was the more accurate value of total mass airflow. A comparison of the trapped air mass calculations is depicted in Figure 7.4. There were no corrections for speed dependencies, or other parameters, in this comparison. This data compares fairly well, with approximately ± 8 percent maximum deviation.

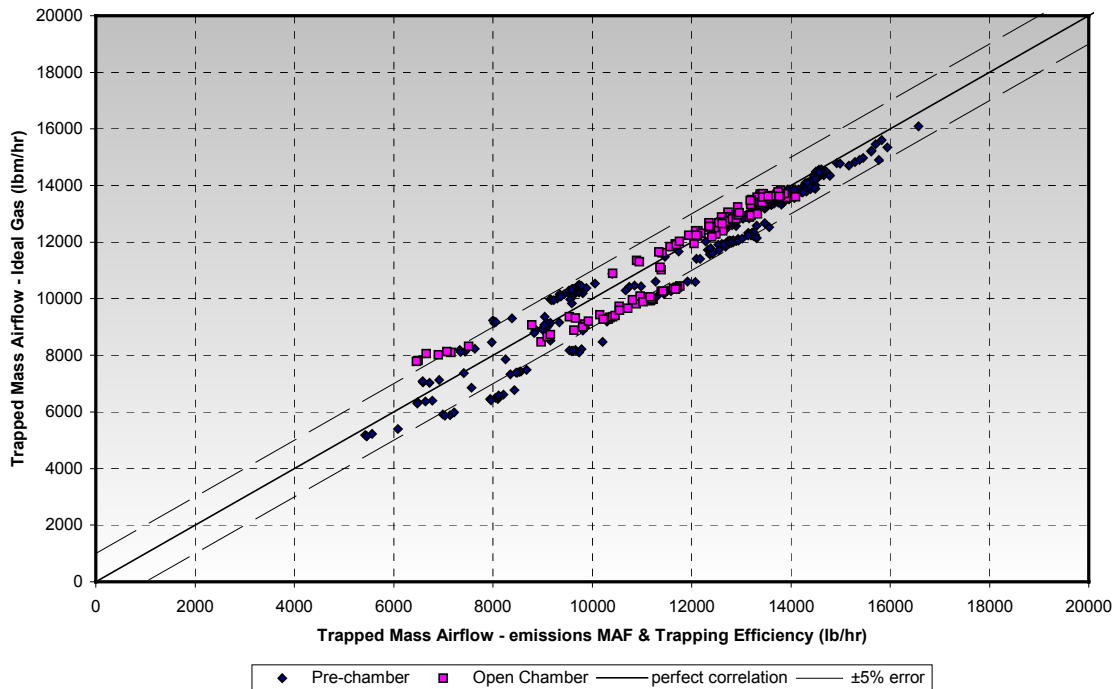


Figure 7.4. Comparison of Dry Trapped Mass Airflows from Trapping Efficiency and Ideal Gas Based Calculations

7.2 Trapped Equivalence Ratio

With the trapped mass airflow predicted, the next analytical step was to estimate the trapped equivalence ratios with methods described in Section 5.3. For this step the air and fuel flows were assumed to be evenly distributed among cylinders. A comparison of the estimated trapping efficiency versus pressure ratio for the data set is provided in Figure 7.5, and shows a range of 50 to 70 percent depending on operating condition. The estimated trapped equivalence ratios from the trapping efficiency based method is shown versus pressure ratio in Figure 7.6.

Estimated trapped equivalence ratios for the PCC is shown in Figure 7.6 to be leaner than with open-chamber, as expected. The lower limit (lean) trapped equivalence ratios for the open-chamber data is approximately 0.535, which were data points acquired near the lean limit. To put this in perspective, data from many tests of open-chamber four-stroke natural gas engines exhibit a lean limit of approximately 0.580. Presuming the equivalence ratios from the four-stroke engine tests are accurate and the lean limit should be comparable, this indicates the trapped equivalence ratio estimates for the two-stroke may contain some error. The upper limit of the open-chamber data in Figure 7.6 were from conditions at or near the knock limit. The PCC data is much tighter due to the lack of test data near the extremes of knock and lean limit.

Estimated trapped equivalence ratios using the ideal gas based method are shown in Figure 7.7 versus pressure ratio. Again, no corrections for speed or other dependencies are included in this data. The values for open-chamber and PCC configurations exhibit more scatter than with the

trapping efficiency based method. The mean values are fairly similar as would be expected with the similar trapped air mass flow estimations shown in Figure 7.4.

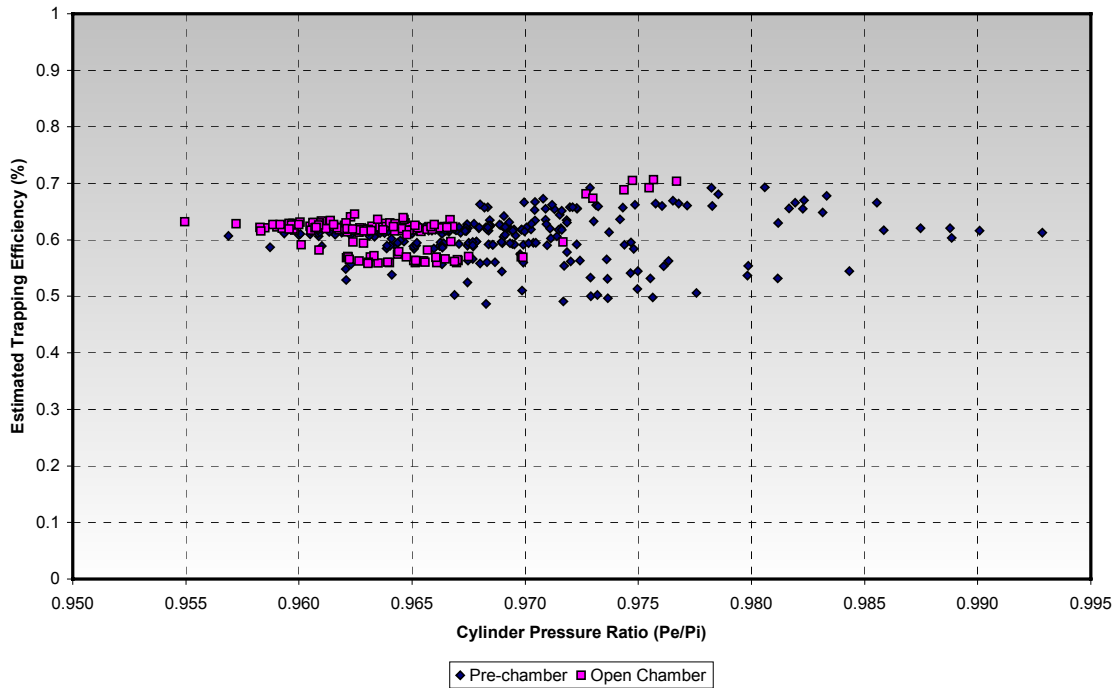
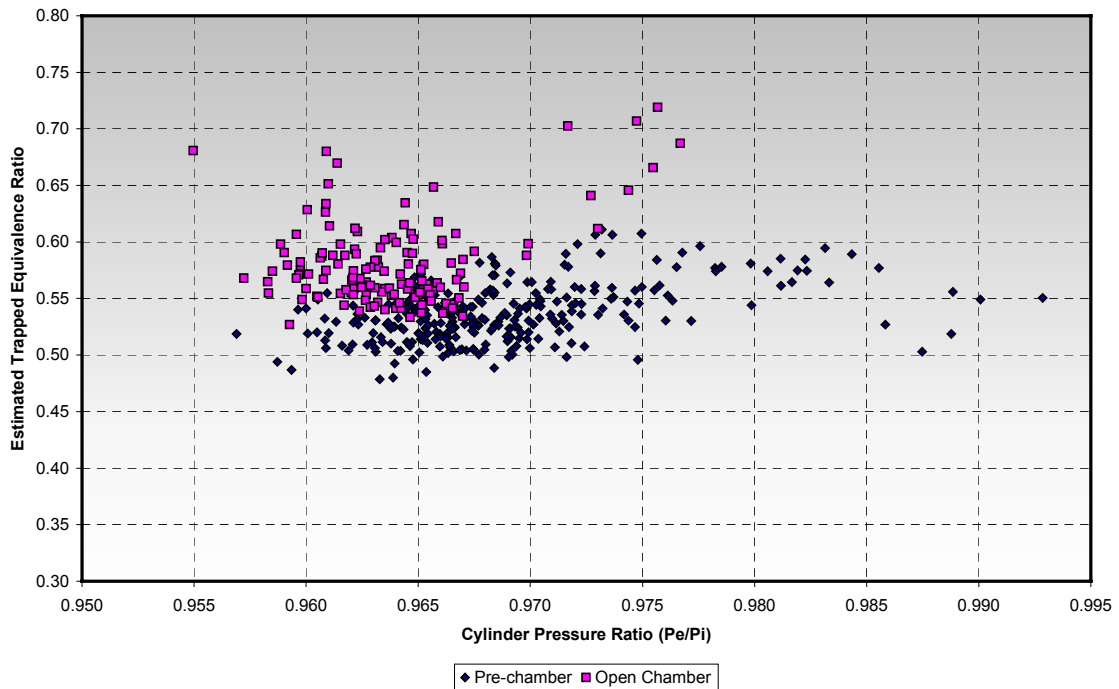


Figure 7.5. Comparison of Estimated Trapping Efficiencies



**Figure 7.6. Estimated Trapped Equivalence Ratios
Using the Trapping Efficiency Based Method**

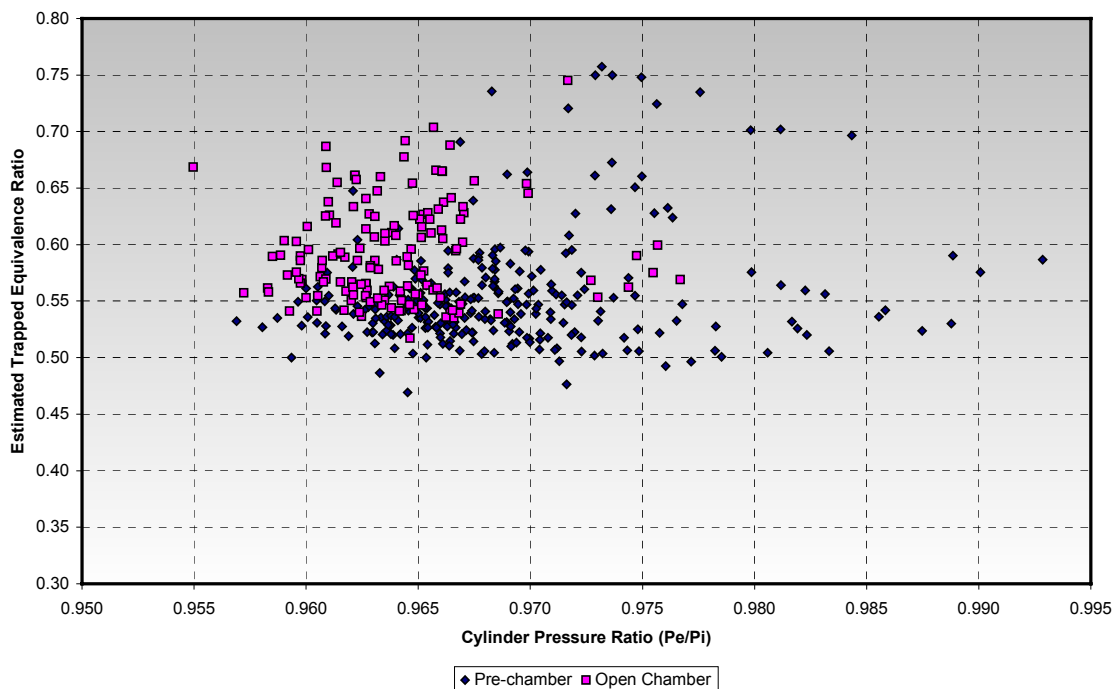


Figure 7.7. Estimated Trapped Equivalence Ratios Using the Ideal Gas Based Method

7.3 NO_x Prediction From Trapped Equivalence Ratio

As described in Section 5.1, a control strategy typically requires some control logic as part of the open-loop control strategy. The control strategies discussed in Section 6.3 are open-loop strategies that utilize trapped equivalence ratio as part of the control logic. A similar approach to these strategies was undertaken to compare the potential open-loop error by a NO_x emissions prediction algorithm from equivalence ratio and other critical parameters. The closed-loop feedback signal from the NGK-Locke sensor could then be used to trim or correct the NO_x prediction algorithm to precisely control engine-out NO_x.

NO_x is primarily a function of combustion temperature and time at that temperature, as discussed in Section 5.4. The primary factors affecting the combustion temperature and time are equivalence ratio, ignition timing, inlet manifold temperature, engine speed, and load. Ambient (or inlet) humidity is also a strong contributor to combustion temperature and NO_x production, and is one parameter that cannot typically be controlled. A regression analysis was conducted with these parameters, as well as others, to determine which offered the best prediction of NO_x emissions. The global equivalence ratio and both of the trapped equivalence ratios were used in three separate regressions with the following parameters:

- Engine Speed
- Ignition Timing

- Air Manifold Temperature
- Air Manifold Pressure (absolute, used for load indicator)
- Specific Humidity

Other parameters were investigated, but no significant improvement in the standard error of regression was realized. It was thought that it would be more appropriate, and provide a better fit, to use combustion phasing (i.e. location of 50 percent mass fraction burn) rather than spark timing. Spark timing can correspond to significantly different combustion affects depending on the engine speed and load. Although a slight improvement in the correlation was realized with combustion phasing, the improvement was not felt significant to justify the requirements of measuring cylinder pressure and performing combustion analysis for a potential control system using this type of strategy.

The result of the empirical NO_x data regression using global equivalence ratio is shown in Figure 7.8. In this figure, the predicted versus measured NO_x is compared for both PCC and open-chamber. The reason for performing this regression with global equivalence ratio was to provide a baseline and determine the error between the global and trapped equivalence ratio values. The global equivalence ratio is also the value that the UEGO sensor would report back to a control system. As seen in Figure 7.8, the regression is not very good and there is significant error in the prediction at all magnitudes of NO_x levels.

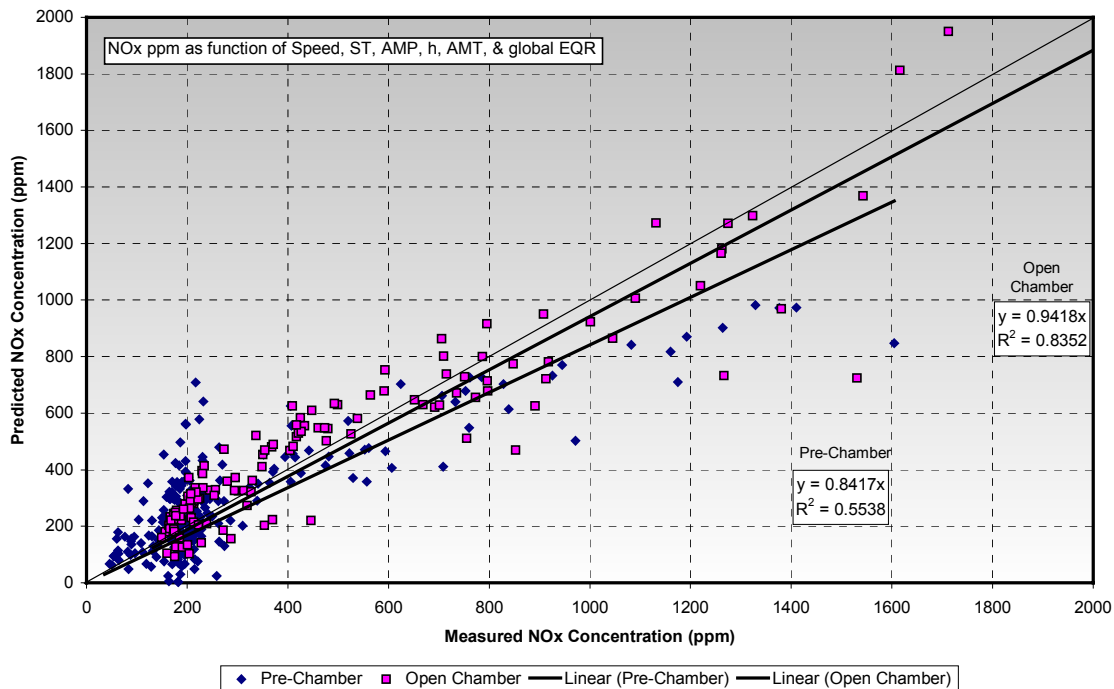


Figure 7.8. Comparison of Predicted versus Measured NO_x with Global Equivalence Ratio Regression

The same regression was performed with the trapped equivalence ratios derived from the trapping efficiency and ideal gas techniques. Results of these regressions are shown in Figures 7.9 and 7.10. In these figures, the comparison of predicted to measured NO_x is greatly improved over the regression with global equivalence ratio. There also is a slight improvement in the fit with the ideal gas based equivalence ratio compared to that based on the trapping efficiency. The regression statistics for all three regressions is provided in Table 7.1 for reference.

Both trapped equivalence ratio regressions included engine speed as one of the parameters, and both regressions were linearly based. Future analysis, assuming this strategy is to be pursued, will investigate non-linear regressions to improve the standard error of the open-loop calculation for NO_x. Published data from researchers employing similar approaches (Section 6.3) have shown NO_x to follow a linear trend for open chamber engines. These same reports show the NO_x to be non-linear with corrected trapped equivalence ratio for engines equipped with PCC [5,9]. The non-linearity with PCC is likely due to an increasing contribution of NO_x from the PCC as the main chamber becomes leaner. For this first iteration, this non-linearity was ignored, as the focus was more on a comparison between trapped equivalence ratio techniques rather than the absolute accuracy of the regression.

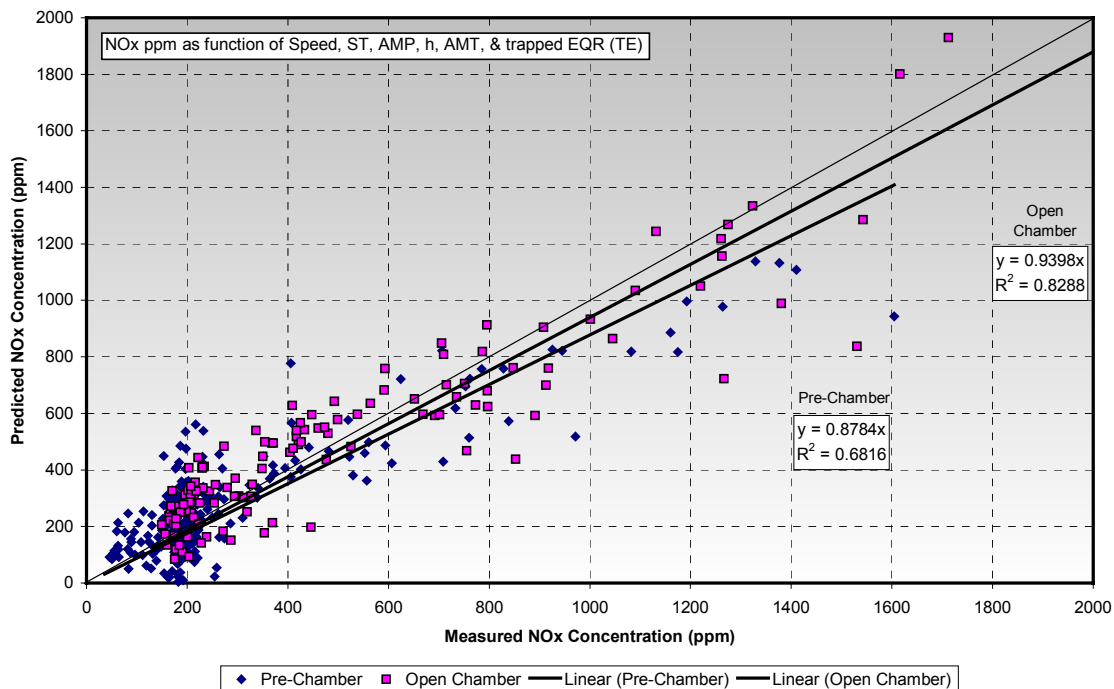


Figure 7.9. Comparison of Predicted versus Measured NO_x with Trapped Equivalence Ratio (Trapping Efficiency Based) Regression

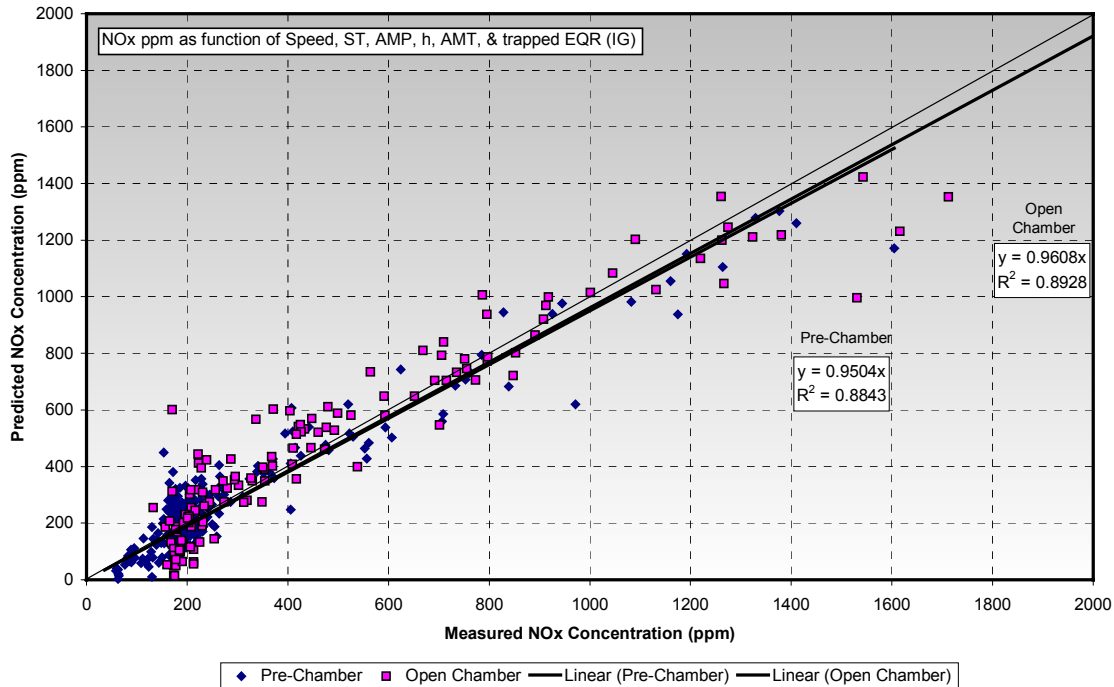


Figure 7.10. Comparison of Predicted versus Measured NO_x with Trapped Equivalence Ratio (Ideal Gas Based) Regression

TABLE 7.1. REGRESSION STATISTICS FOR EQUIVALENCE RATIO BASED NO_x PREDICTION

Statistic	Global EQR		Trapped EQR (Trapping Eff. Based)		Trapped EQR (Ideal Gas Based)	
	Open Chamber	Pre-Chamber	Open Chamber	Pre-Chamber	Open Chamber	Pre-Chamber
R ²	0.85	0.65	0.89	0.79	0.90	0.89
Std Error	155.3	146.2	131.7	114.1	129.7	83.8

7.4 Modified Fuel-Air Curve

The fuel-air curve described in Section 6.1 was not originally felt sufficient for accurate control of NO_x emissions. However, it may be possible to modify the technique to prevent large corrections by the closed-loop feedback signal from the NGK-Locke sensor. This approach will be pursued in the second half of the program.

7.5 Cylinder Pressure Based NO_x Prediction

Analysis of the cylinder pressure, or combustion temperature, based methods described in Sections 5.4 and 6.4 will be conducted in the second half of this project. The equations in Section 5.4 will be applied with the measured data to determine if this approach provides

significant benefits over the trapped equivalence ratio techniques. This method will require the use of continuous cylinder pressure measurement to be implemented, which is a significant hardware requirement compared to other control approaches.

7.6 Individual Cylinder Based Strategies

An investigation into the feasibility of performing individual cylinder control will be conducted in the second half of this program. The sensor and processor requirements of such a system will be outlined as part of this task. This type of strategy is felt to be the most optimum approach for accurate control of NO_x emissions with best fuel efficiency. The use of cylinder pressure measurements along with combustion parameters will be required for this strategy.

8. CONCLUSIONS

The use of the NGK-Locke combined O₂/NO_x sensor for closed-loop feedback signals can apply to virtually all open-loop controls strategies being used for integral compressor engines today. There may be, however, limitations it's use with some strategies due to the large error for acceptable control. This concern led to the review of current control strategies and the accuracy of common NO_x control methods using data generated from the GMVH laboratory engine.

It is envisioned that a hierarchy of control strategies will be outlined at the conclusion of this program. This hierarchy will range from the simplest and least expensive closed-loop control to an advanced system utilizing individual cylinder control. Use of the NGK-Locke sensor for closed-loop feedback with other open-loop control strategies will be outlined.

REFERENCES

1. Palm, William, Modeling, Analysis, and Control of Dynamic Systems, John Wiley & Sons, 2000. Page 449.
2. Heywood, John, Internal Combustion Engine Fundamentals, McGraw-Hill Publishing Company, 1988.
3. Society of Automotive Engineers, Recommended Practice, J1829, 2002.
4. Taylor, C.F., The Internal Combustion Engine in Theory and Practice, Vol. 1, 2nd ED., MIT Press, 1985.
5. "Enhanced Monitoring Protocol Guidelines for IC Engine Parameter Based Compliance Monitoring Systems," PRCI Final Report, Contract No. PR-239-9439, 1997.
6. Stone, Richard, Introduction to Internal Combustion Engines, Society of Automotive Engineers, 1999.

7. Wood, C.D., et al, "Evaluation of Emissions Control Technology for Reciprocating Integral Engine-Compressor Units," SwRI Final Report for Tenneco Gas Environmental and Technology Department, 1995.
8. Kubesh, J. and Liss, W., "Simple NO_x Model for Predictive Emissions Monitoring," ASME Paper ICE-Vol. 21, 1994.
9. Beshouri, G.M., "Combustion Pressure Based Emissions Monitoring and Control for Large Bore IC Engines – An Alternative Parametric Emissions Model (PEM) Methodology," ASME Paper, 1998.
10. Kato, N., Nakagaki, K., and Ina, N., "Thick Film ZrO₂ NO_x Sensor, SAE Paper No. 960334, February 1996.
11. Kato, N., Hamada, Y., and Kurachi, H., "Performance of Thick Film NO_x Sensor on Diesel and Gasoline engines, SAE Paper No. 970858, February 1997.
12. Kato, N., Kurachi, H., and Hamada, Y., "thick Film ZrO_x NO_x Sensor for the Measurement of Low NO_x Concentration", SAE Paper No. 980170, February 1998.
13. Kato, N., Kokune, N., Lemire, B. and Walde, T., "Long Term Stable NO_x Sensor with Integrated In-Connector Control Electronics", SAE Paper No. 199-01-0202, March 1999.
14. Malicke, D. and Mathews, H., "Equivalence Ratio Based Air/Fuel Ratio Control Strategies," Gas Machinery Conference, October, 6, 2003.
15. Beshouri, G. and Matthews, H., "Designing Engine Retrofits for Emissions Reduction," Gas Machinery Conference, October, 2002.
16. Brooks, M., "Enginuity Technologies Complete First Ever Low-Emissions Combustion Retrofit of Ingersoll-Rand KVG Engine-Compressor," Compressor Tech Magazine, November-December, 1999.
17. Smith, J., "Integration Of Engine And Compressor Controls", SwRI Report to Gas Machinery Research Council, May, 2002.
18. Bourn, G., "Identification of Compressor Load-Step on NO_x Emissions and Efficiency," SwRI Internal Research Final Report, 2002.